Published in final edited form as:
Eur J Neurosci. 2010 September ; 32(5): 693–706. doi:10.1111/j.1460-9568.2010.07337.x.

Requirement of cannabinoid CB_1 receptor in cortical pyramidal neurons for appropriate development of corticothalamic and thalamocortical projections

Chia-Shan Wu[1], **Jie Zhu**[1], **Jim Wager-Miller**[3], **Shan Wang**[1], **Dennis O'Leary**[4], **Krisztina Monory**[5], **Beat Lutz**[5], **Ken Mackie**[3], and **Hui-Chen Lu**[1,2]

[1]Department of Pediatrics, Baylor College of Medicine, Houston, TX

[2]Department of Neuroscience and Program in Developmental Biology, Baylor College of Medicine, Houston, TX

[3]Gill Center and Department of Psychological and Brain Sciences, Indiana University, Bloomington, IN

[4]Salk Institute, San Diego, CA

[5]Institute of Physiological Chemistry, University Medical Center of the Johannes Gutenberg University, Mainz, Germany

Abstract

A role for endocannabinoid signaling in neuronal morphogenesis as the brain develops has recently been suggested. Here we used the developing somatosensory circuit as a model system to examine the role of endocannabinoid signaling in neural circuit formation. We first show that deficiency of cannabinoid receptor type 1 (CB_1R), but not G-protein coupled receptor 55 (GPR55), leads to aberrant fasciculation and pathfinding in both corticothalamic and thalamocortical axons despite normal target recognition. Next, we localize CB_1R expression to developing corticothalamic projections, and find little if any expression in thalamocortical axons, using a newly established reporter mouse expressing GFP in thalamocortical projections. A similar thalamocortical projection phenotype is observed following removal of CB_1R from cortical principal neurons, clearly demonstrating that CB_1R in corticothalamic axons is required to instruct their complimentary connections, thalamocortical axons. When reciprocal thalamic and cortical connections meet, CB_1R-containing corticothalamic axons are intimately associated with elongating thalamocortical projections containing DGLβ, a 2-arachidonoyl glycerol (2-AG) synthesizing enzyme. Thus, 2-AG produced in thalamocortical axons and acting at CB_1Rs on corticothalamic axons is likely to modulate axonal patterning. The presence of MGL, a 2-AG degrading enzyme, in both thalamocortical and corticothalamic tracts likely serves to restrict 2-AG availability. In summary, our study provides strong evidence that endocannabinoids are a modulator for the proposed handshake interactions between corticothalamic and thalamocortical axons, especially for fasciculation. These findings are important in understanding the long-term consequences of alterations in CB_1R activity during development, a potential etiology for the mental health disorders linked to prenatal *Cannabis* use.

Keywords

neural circuit; endocannabinoids; ECS; cortex; thalamus

Corresponding Author: Hui-Chen Lu, Baylor College of Medicine, 1102 Bates St. Feigin Center, MC3-6365, Houston, TX 77030, Tel: 832-824-3966; Fax: 832-825-4217, hclu@bcm.edu.

Introduction

Human epidemiological and animal studies consistently find that early cannabis exposure influences brain development and can have long-lasting impacts on cognitive functions (Navarro *et al.*, 1994; Navarro *et al.*, 1995; Richardson *et al.*, 2002; Mereu *et al.*, 2003; Smith *et al.*, 2004; Antonelli *et al.*, 2005; Campolongo *et al.*, 2007; Spano *et al.*, 2007; Smith *et al.*, 2006). Cannabis produces most of its effects by interacting with cannabinoid receptors. The endocannabinoid system (ECS) consists of endogenous cannabinoids (eCBs), their receptors (CB_1R, CB_2R, possibly GPR55 and others), and the enzymes responsible for the synthesis and degradation of eCBs (for reviews, see Lutz, 2002; Freund *et al.*, 2003; Iversen, 2003; Chevaleyre *et al.*, 2006; Kano *et al.*, 2009). Despite a wealth of knowledge on the role of eCB signaling in mature neural circuits, an appreciation of its role in embryonic development is just unfolding (Harkany *et al.*, 2008). A detailed understanding of how ECS signaling modulates specific aspects of brain development will be critical to understanding the detrimental impact of prenatal and early postnatal cannabis exposure.

Thalamic axons projecting into the cortex provide the majority of cortical sensory input, while reciprocal innervations from the cortex to the thalamus send critical feed-back to modulate the thalamic responses required to perform the complex information processing and integration that underlie cognitive behaviors (Jones, 2002; Alitto & Usrey, 2003; Temereanca & Simons, 2004; Theyel *et al.*, 2010.). The development of these sensory circuits is critically sensitive to sensory experience, pathological conditions, and drugs of abuse (Feldman & Brecht, 2005; Hensch, 2005; Sur & Rubenstein, 2005; Feldman, 2009; Heath & Picciotto, 2009). The proper development of these long-range, complementary connections between a unique set of thalamic nuclei and a particular cortical area requires an elaborate coordination of multiple factors that initiate and guide axon outgrowth, fasciculation, navigation, target recognition, and refinement (Katz & Constantine-Paton, 1988; Molnar *et al.*, 2003; Garel & Rubenstein, 2004). A “handshake hypothesis” for thalamocortical axons (TCAs) and corticothalamic axons (CTAs) interactions has been postulated based on the close association of these tracts (Molnar & Blakemore, 1995; Molnar *et al.*, 1998a), the inverted TCA pattern in *reeler* mouse (Molnar *et al.*, 1998b), and by the observation that deleting a particular transcription factor expressed only in the cortex or only in the thalamus leads to abnormalities of both tracts (Hevner *et al.*, 2002). However, the underlying mechanisms for the interdependence between TCAs and CTAs are unclear.

The abnormal axonal fasciculation found in the cannabinoid receptor type 1 (CB_1R) knockout (KO) mice (Mulder *et al.*, 2008) led us to hypothesize that eCB signaling modulates the formation of neural circuits. Here we examined TCA and CTA projections in complete CB_1R KO (Marsicano *et al.*, 2002), in conditional CB_1R KO lacking CB_1R in cortical glutamatergic neurons (Monory *et al.*,, 2006), and GPR55 KO mice. Immunohistochemistry was conducted to examine the distribution of specific ECS components in the developing brains. Our data suggest that ECS signaling is one of the modulators of the “handshake” interactions between TCAs and CTAs.

Materials and Methods

Animals

The generation and genotyping of CB_1R total and NEX- CB_1R ($CB_1R^{f/f;NEX\text{-}Cre}$) conditional knockout mice and their littermates have been described (Marsicano *et al.*, 2003; Monory *et al.*, 2006). GPR55 knockout mice were acquired from the Texas Institute of Genomic Medicine (Houston, TX) and were maintained on a mixed C57BL/6-Sv129 genetic background (see Supplementary Materials and Sup. Fig. 1 for details of their generations).

Tau^{mGFP} mice is a Cre-reporter line containing a floxed "stop transcription" sequence in front of membrane anchored GFP (mGFP) and an IRES-NLS-lacZ gene inserted into exon 2 of the Tau locus (Hippenmeyer et al 2005). Cre mediated recombination can be detected by the presence of nuclear β-galactosidase, because of the nuclear localization sequence (NLZ) engineered in the LacZ gene, and by the expression of mGFP in the axons of recombined neurons. RORα-Cre mice were generated by inserting an *IRES-cre* cDNA fragment into the 3' noncoding region of the RORα gene in Dr. Dennis O'Leary's laboratory (data not shown). Cre expression in RORα-Cre mice is similar to endogenous *ROR*α expression (Nakagawa & O'Leary, 2003). TCA^{GFP} mice were obtained from the F1 progeny of the crossing between $ROR\alpha^{Cre/+}$ and $Tau^{mGFP/+}$ mice (see Supplementary Materials and Sup.Fig. 2).

Mouse colonies were maintained in a pathogen-free environment on a 12 hr light:dark cycle. Both CB_1R and GPR55 mice were bred by mating heterozygous females to heterozygous or homozygous males. Since TCA and CTA development in CB_1R heterozygotes are indistinguishable from wild type mice, both wild type and CB_1R heterozygotes were used as controls in these studies. The day of vaginal plug was designated as E0.5, and the day of birth as P0.

All experiments and data analysis were done blinded to genotype. For genotyping, tail lysates were prepared by immersing tail pieces in 50 mM NaOH, boiling for 30 minutes, vortexing vigorously for 10 sec, and then neutralizing with 1M Tris-HCl (pH8.0). Tail lysates were then vortexed for another 10 sec and centrifuged at 16,100 g for 1 minute. The supernatants were used as DNA templates for polymerase chain reaction (PCR) reactions. For GPR55, PCR reactions were conducted with a mixture of two primer pairs. The PCR products were 441 bp for the wt GPR55 allele and 301 bp for the neo allele. The primer sequences were: 5' – GCCATCCAGTACCCGATCC – 3' and 5' – GTCCAAGATAAAGCGGTTCC – 3' for the wt allele; 5' – GCAGCGCATCGCCTTCTATC – 3' and 5' – TCAAGCTACGTTTTGGGTT – 3' for the GPR55 mutant allele. For RORα-Cre, PCR reactions were conducted with a mixture of primers ROR-1 and ROR-2. The PCR products were 500 bp. The primer sequences were: ROR1: 5'- GAT CTC CGG TAT TGA AAC TCC AGC -3'; ROR2: 5'- GCT AAA CAT GCT TCA TCG TCG G -3'. For Tau^{mGFP} mice, PCR reactions were conducted with a mixture of primers GFP-1 and GFP-2. The PCR products were 500 bp. The primer sequences were: GFP1: 5'- CGG CGA GGG CGA GGG CGA TG -3'; GFP2: 5'- CAG GGG GCC GTC GCC GAT GG -3'. Animals were treated in compliance with the U.S. Department of Health and Human Services and Baylor College of Medicine guidelines.

Antibodies

The following antibodies were generated in the laboratory of Dr. Ken Mackie: guinea pig CB_1R antibody (Ab) (against the C-terminus AA400–473; 1.5 μg/ml); rabbit anti-DGLβ (against AA 205–287;5μg/ml), rabbit anti-MGL (against AA 171–206; 1.5 μg/ml). Antibody specificity was validated by one or more of the following methods: (1) lack of staining in corresponding knockout mice (CB_1R, Mulder et al., 2008 and our data not shown), (2) identical staining patterns by two different primary antibodies directed against distinct epitopes within a target protein (DGLβ, Berghuis et al., 2007; MGL, personal communication with T. Harkany), (3) co-localization with V5-tagged target protein heterologously expressed in HEK293 cells (MGL, Straiker *et al.*, 2009). The staining pattern of MGL in hippocampus in P7 mouse brain is similar to a previous report using a MGL Ab raised against mouse MGL AA 21–35 (Dinh *et al.*, 2002). The CTFL antibody characterized in this study as a TCA marker was raised against the full C-terminal of mouse GPR55 (KEFRMRIKAHRPSTIKLVNQDTMVSRG) (Lauckner *et al.*, 2008; see Supplementary Materials and Sup. Fig. 3). Rat anti-L1 antibody (1:1000) was purchased from Millipore

(Temecula, CA), and chicken anti-GFP (1:1000) was purchased from Aves Labs (Tigard, OR). Secondary antibodies (companies and dilutions): biotinylated goat anti-guinea pig IgG (Jackson Immunoresearch Laboratories, West Grove, PA; 1:500); goat anti-rabbit IgG-Alexa 488 (Molecular Probes, 1:500); goat anti-rat IgG-Alexa 488 (Molecular Probes, 1:500); goat anti-chicken IgG-Alexa 488 (Molecular Probes, 1:500); goat anti-guinea pig IgG-Alexa 647 (Molecular Probes, 1:500); and goat anti-rabbit IgG-Cy3 (Jackson Immunoresearch Laboratories, 1:500). No immunoreactivity was detected when the primary antibodies or the secondary antibodies were omitted from the staining procedure.

Tissue preparation

Postnatal mice were deeply anesthetized with an injection (i.p.; 3 ml/kg) of a rodent anesthetic cocktail containing ketamine 37.6 mg/ml, xylazine 1.92 mg/ml and acepromazine 0.38 mg/ml. Following establishment of anesthesia, mice were transcardially perfused with ice-cold phosphate buffered saline (PBS), pH 7.4, followed by 4% paraformaldehyde (PFA) in PBS, pH 7.4. The brains were then post-fixed with the same fixative overnight at 4°C. Brains from E14.5 and E16.5 embryos were removed and fixed in 4% PFA at 4°C. Following overnight fixation, all brains were washed with PBS and stored in PBS/0.1% sodium azide at 4°C until processing.

DiI-labeling experiments

Labeling of axonal tracts with the lipophilic carbocyanine dye DiI (1,1'-diotadecyl-3,3,3',3'-tetramethylindocarbocyanine; Molecular Probes, Eugene, OR) was performed in fixed E16.5-P4 brains. A single crystal of DiI was picked up on a fire-polished tip of a broken glass micropipette and inserted into the presumptive primary somatosensory cortex, or into the dorsal thalamus or the ventral basal thalamus (exposed by a cut anterior to the cerebellum), for corticothalamic and thalamocortical labeling, respectively. The DiI-containing brains were incubated in PBS/0.1% sodium azide at 50°C in the dark for 2 weeks. Brains were then embedded in 3% agar and sectioned at 100 μm in the coronal plane using a Leica VT1000S vibrating microtome (Leica Microsystems, Bannockburn, IL). Axon projections were visualized using a conventional fluorescence microscope (Zeiss AxioImager M1 with 5× / 0.16 and 10× / 0.3 Zeiss objectives) and a laser-scanning confocal microscope (Leica DM confocal scanning microscope, 10× / 0.4, 63× / 1.2 /water immersion).

Immunohistochemistry with the peroxidase ABC method

Brains were sectioned into 50 μm thick-sections with a Leica VT1000S vibrating microtome in the coronal plane. These tissue sections stayed free-floating for all subsequent washings and incubations. Free-floating sections were washed with PBS and then permeabilized with 0.2% Triton X-100 in PBS, pH7.4, at room temperature for 10 minutes. To reduce endogenous peroxidase activities, sections were treated with 3% H_2O_2, 10% methanol in 0.2% Triton X-100 in PBS at room temperature for 5 minutes. Sections were then washed with PBS with 0.01% Triton X-100 (PBST) and blocked with 3% normal goat serum in PBST at room temperature for one hour. Subsequently, sections were incubated with guinea pig anti-CB_1R Ab in PBST with 2 mg/ml BSA and 1% normal goat serum at 4 ° C overnight. After repeated washes with PBST, sections were incubated with 1:500 biotinylated goat anti-guinea pig IgG in PBST for one hour. After repeated washes with PBST, sections were further incubated for 1 hour with avidin-biotinylated peroxidase complex (ABC; Standard VECTASTAIN® ABC kit, Vector Laboratories, Burlingame, CA) in PBST. Following ABC amplification, diaminobenzamide (DAB) signals were developed with Vector DAB substrate kit (Vector). During this staining step, the staining intensity was examined under Zeiss Stenu DV4 8–32× dissection microscope and the reactions were stopped when clear immunoreactivity was detected. Stained sections were then mounted

onto Superfrost Plus slides (Fisher Scientific), dehydrated in gradual ethanol series, cleared in xylene, cover-slipped with Cytoseal mounting medium (Richard Allen Scientific, Kalamazoo, MI), and imaged by bright field microscopy.

Multiple antibody immunofluorescence staining

Free-floating sections were washed with PBST and permeabilized with 0.2% Triton X-100 in PBS at room temperature for 20 minutes. Sections were then washed with PBST, blocked for one hour with 3% normal goat serum in PBST at room temperature, and then incubated with a mixture of two primary antibodies from different species in PBST with 2 mg/ml BSA and 1% normal goat serum at 4°C overnight. The next day, sections were washed with PBST, and incubated with the appropriate fluorescent secondary antibodies in PBST at room temperature for two hours. Following this incubation, sections were washed with PBST for three times for 10 minutes each. After DAPI staining, sections were mounted and cover-slipped for imaging.

Imaging

Bright field images were captured from an Olympus BX51 upright microscope with 2× / 0.08 Plan Apo, 4×/ 0.16 UPlan Apo objectives (magnification / numerical aperture), using an Olympus DP70 CCD camera with Olympus DPC controller software. Fluorescent images were obtained using Zeiss AxioImager M1 system with 5× / 0.16, 10×/ 0.3 Zeiss objectives, using AxioVision software. Confocal images were obtained using a Zeiss 510 system 10× / 0.45 (air), 16× / 0.5, 40× / 1.3 and 63× / 1.4 / oil immersion objective lens. Alexa 488, Cy3, or Alexa 647 fluorophores were excited with lasers of appropriate excitation wavelength (488 nm, 543 nm, or 633 nm) and scanned with emission filters selected to optimally separate fluorescence (510/530 band pass filter for Alexa 488; 560/600 band pass filter for Cy3; 660 long pass filter for Alexa 647). Each image was acquired with the laser intensity adjusted to prevent saturation. High-resolution (~200 nm) images were taken with a 63× oil immersion lens (N.A. 1.4) with 2× zoom on the Zeiss 510 confocal system. This resolution is at the detection limit of standard confocal laser scanning system (Heintzmann & Ficz, 2006). For co-localization of immunosignals, high magnification images were taken with pin hole sizes set to give an optical thickness of less than 1 μm for all channels. All images were processed as a whole in Adobe Photoshop CS2 (San Jose, CA) for brightness/contrast, orientations, and background corrections to better illustrate the staining patterns. Regions of interest in digital images were copied and assembled into montages with Adobe Illustrator (San Jose, CA). Cytoarchitectonic areas and fiber tracts were annotated based on the Atlas of the Developing Mouse Brain (Jacobowitz & Abbott, 1998).

Morphometric analysis and statistics

Coronal sections of E16.5 embryonic brains stained for CTFL were analyzed using a 10×objective (NA = 0.3) on an Apotome (medium grid)-equipped Zeiss AxioImager M1. Exposure time was adjusted to avoid saturations. At least two comparable coronal sections separated by > 200 μm in rostrocaudal axis at the planes illustrated in Fig. 1A were imaged for each animal. Z-stacks of 10 optical slices (5 slices above and below the middle focal plane of the section) with 1.52 μm optical thickness were captured for the PSPB area in each hemisphere. During staining, the thickness of sections shrank from 50 μm to ~20 μm, so this distance (~15 μm) covers most of the axon fascicles present in the area imaged. For morphometric analysis of fascicle size and density, image stacks were collapsed using the maximum projection function in ImageJ. The diameter of all axon fascicles present in an area of 100 μm × 400 μm (dotted box in Fig. 3C and D), located 100 μm away from the pallial-subpallial border demarcated by DAPI counterstaining (yellow dotted line in Fig. 3C and D), were measured as described (McIlvain *et al.*, 2003). Three to five PSPB areas were analyzed for each mouse brain, and data from each animal were averaged into one data

point. Fascicle size and density (number of fascicles per defined area measured) derived from wild-type and CB_1R KO mice were compared using non-directional student's t-test. A $p < 0.05$ was considered statistically significant (SigmaStat 3.5, Systat Software, Inc.). Data were presented as mean ± SEM. For the distribution and cumulative comparison graphs, the data from individual fascicles derived from CB_1R KO and littermate control sections were pooled. All graphs were plotted using SigmaPlot 10 (Systat Software, Inc.).

Results

CB_1R loss-of-function leads to aberrant axonal fasciculation in both the thalamocortical and corticothalamic projections

CB_1Rs are involved in axonal pathfinding and fasciculation (reviewed in Harkany *et al.*, 2008). To specifically explore the role of CB_1R in the development of the corticothalamic and thalamocortical projections, we examined these projections in CB_1R knockout and their littermate control mice. To do this, the lipophilic carbocyanine dye, DiI, was placed into the presumptive primary somatosensory (S1) region to label CTAs or into the dorsal thalamus to label TCAs (Fig. 1). In rodents, the thalamocortical axons (TCAs) first project ventrally and then turn about 90 degree at the boundary between the diencephalon and the telencephalon to enter the internal capsule as tight bundles (Molnar *et al.*, 1998b; Lopez-Bendito & Molnar, 2003; Price *et al.*, 2006). Once they reach the striatum proper, TCAs spread out into multiple fascicles and navigate towards the cortical plate. However, their migration pauses at the pallial-subpallial boundary (PSPB) at E14.5 (Molnar and Cordery, 1999). Correspondingly, corticothalamic axons (CTAs) originate from preplate pyramidal neurons, leave the cortex and transiently pause at the PSPB at E14.5 (Molnar & Cordery, 1999; Jacobs *et al.*, 2007). After a period of interaction between TCAs and CTAs, each resumes their progression toward their specific targets (Molnar *et al.*, 1998a; Molnar & Cordery, 1999).

In both CB_1R KO (n = 7) and control (n = 12) E16.5 brains, DiI-labeled CTAs navigated through the intermediate zone of the cortical plate, the PSPB, and traversed the striatum (Fig. 1 C1, D1). They then passed through the internal capsule and reached the thalamus (Fig. 1 C2, D2). Despite the rather normal innervation path and correct targeting, abnormally large CTA fascicles were often found in the striatum close to the PSPB boundary in CB_1R KO mice (Fig. 1 D1).

The thalamocortical projections labeled by DiI in both CB_1R KO (n = 5) and control (n = 10) E16.5 brains were found as tight bundles in the internal capsule and fascicle arrays in the striatum (Fig. 1 E1, E2, F1, F2). The majority of DiI-labeled TCAs in CB_1R KO mice and almost all TCAs in the littermate control mice turned dorsomedially into the cortical plate once they passed through the PSPB. However, in CB_1R KO PSPB, many misrouted TCAs extended ventro-laterally first before turning dorsal-medial directions and entering the cortical plate to meet up with the rest of TCAs (Fig. 1F). Also, abnormally large TCA fascicles were found in the striatum near PSPB and the subplate area of the cortical plate of CB_1R mutant KO mice (Fig. 1F). Taken together these results suggest that CB_1Rs are necessary for fascicles to appropriately organize in both corticothalamic and thalamocortical projections but CB_1Rs are not required for general target recognition.

Based on its activation by the cannabinoid receptor agonists Δ^9-tetrahydrocannabinol (THC) and anandamide (one of the two major eCBs), GPR55, a member of the G protein-coupled receptor (GPCR) superfamily was proposed to be a cannabinoid receptor (Lauckner *et al.*, 2005; Ryberg *et al.*, 2007). In addition, GPR55 mRNA is expressed in brains (Sup. Fig. 1C), leading us to speculate that GPR55 might have a role in axonal pathfinding. Thus, DiI-tracing was conducted to examine corticothalamic and thalamocortical projections in GPR55

KO mice (Fig. 2; see Sup. Fig. 1 for a description of the generation of these GPR55 KO mice). The patterns of DiI-labeled CTAs and TCAs in GPR55 KO mice (n = 4 for CTAs and n = 4 for TCAs) were similar to their wild type littermates (Fig. 2; n = 4 for CTAs and n = 3 for TCAs). In GPR55 KO brains, both CTAs and TCAs projected into their correct target zones and had normal fasciculation. Thus, GPR55 is not required for the development of thalamocortical and corticothalamic projections.

DiI incorporates into cell membranes and labels neural circuits in both an antero-and retrograde manner. The complementary patterns of DiI-labeled TCAs and CTAs as well as the small number of DiI-labeled thalamic cells after CTA-labeling suggest that the majority of DiI-labeled axons observed likely resulted from anterograde-labeling. However, we cannot rule out that some DiI-positive thalamic cells were retrogradely labeled through the TCAs reaching the cortical plate.

Thalamocortical axon labeling and quantification of aberrant fasciculation in CB_1R KO mice

To verify the aberrant fasciculation phenotype in CB_1R KO mice, we performed double staining with L1-NCAM (L1) and CTFL antibodies (a novel TCA marker; see Materials and Methods and Sup. Fig. 3) in E16.5 CB_1R KO (n = 3) and their littermate control mice (n = 3). The cell adhesion molecule L1 labels both CTAs and TCAs (Jones *et al.*, 2002; Lopez-Bendito *et al.*, 2002), while CTFL immunoreactivity reveals TCAs from E14.5 until P8 (see Sup. Fig. 3). Both L1 and CTFL labeled axon bundles in the PSPB and the fibers traversing the striatum (Fig. 3). The great majority of CTFL-positive fibers were co-labeled with L1 immunoreactivity, while a significant fraction of L1-positive fibers were devoid of CTFL staining (Fig. 3 A, B). The enlarged fascicles and misrouted axon phenotypes in the PSPB area of CB_1R KO brain were observed by both L1 and CTFL staining (Fig. 3B). We quantified the TCA fasciculation deficits in CB_1R KO by measuring the number and the width of individual CTFL-positive fascicles distributed in the PSPB area. To unambiguously compare similar areas among animals, we chose to quantify a rectangular area of 400 μm by 100 μm located within the subpallium, which was 100 μm away from the pallium/subpallium border and readily demarcated by DAPI staining. This area covered the passage of the majority of CTFL-positive fibers traversing the PSPB. The morphometric analysis was conducted in 3–5 different zones per animal and 3 animals per genotype (see Fig. 3 C, D and Materials and Methods). In CB_1R KO mice, there were more TCA fascicles with a diameter larger than 25 μm while very few of control TCA fascicles had a diameter greater than 20 μm (Fig. 3E). More than 50% of CB_1R KO fascicles had a diameter greater than 14 μm, while 50% of control fascicles had diameters under 8 μm (Fig. 3F). The mean fascicle diameter was significantly increased in CB_1R KO mice compared to their littermate controls (Fig. 3H; control: 10.2 ± 1.25 μm, n = 3; KO: 19.0 ± 2.4 μm, n = 3; p = 0.031 by student's *t*-test). Correspondingly since fascicle size was increased, the density of fascicles was significantly reduced in CB_1R KO mice (Fig. 3G; control: 5.8 ± 0.4 fascicles per 10,000μm^2, n = 3; KO: 3.8 ± 0.4 fascicles per 10,000μm^2, n = 3; p = 0.022 by student's *t*-test). Taken together, CB_1R KO mice have fewer, but larger TCA fascicles in the PSPB area.

The defect in thalamocortical development in CB_1R KO mice persists postnatally

To examine whether the aberrant TCA tract formation observed in CB_1R KO mice during embryonic development was transient or persisted postnatally, CTFL immunostaining was conducted using P0-P7 postnatal brains from CB_1R KO mice and their littermate controls (Fig. 4 A–H). Aberrant fasciculation and misrouted axon phenotypes were found in the white matter, the striatum, and the cortico-striatal junction of CB_1R KO mice at P0, P1, P4 and P7. Abnormally large TCA fascicles in P1–7 CB_1R KO mice (ctrl: n = 1 for P0, n = 2

for P1, n = 3 for P4, n = 3 for P7; KO: n = 3 for P0, n = 2 for P1, n = 3 for P4, n = 3 for P7) confirmed that the abnormal TCA phenotype persisted postnatally. DiI tracing was conducted with P1 brains and a similar TCA phenotype was observed (Fig. 4 I, J; n = 3 for ctrl and n = 3 for KO). Interestingly, the degree of axonal fasciculation abnormalities at the postnatal ages examined is very similar to that seen at E16.5. Thus, the developmental structural deficits seen at E16.5 in CB_1R KO TCAs are not corrected by postnatal compensatory mechanisms, at least during the first postnatal week.

Despite these abnormalities, CB_1R KO TCAs reach the cortex and innervate cortical layer IV neurons (Fig. 4E, F and data not shown). At P0, CTFL-positive fibers were found in the internal capsule, the striatum, the white matter, and the deep layers of the cortical plate in both control and CB_1R KO mice (Fig. 4 A, B). At P1, distinctive TCA arborizations in both cortical layer VI and the presumptive layer IV area were observed in the S1 cortex of control and CB_1R KO mice. At P4, whisker-related TCA clusters were evident in the cortical layer IV for both groups of mice (Fig. 4E and data not shown). Deshmukh et al. (2007) also showed a complete whisker-related pattern in the S1 cortex of CB_1R KO mice despite the widening of the septa area between whisker-related TCA clusters. Taken together, the prior results and the present study show that CB_1R function is not required for the general development of cortical sensory map topography.

A complete endocannabinoid signaling system is present in the developing thalamocortical circuit

The presence of functional CB_1Rs in developing white matter areas containing the axons of glutamatergic neurons was first reported using ^3H-labeled-cannabinoid ligands and agonist-induced GTPγS binding (Fernandez-Ruiz *et al.*, 2000). Immunohistochemistry with CB_1R-specific antibodies later confirmed the presence of CB_1R on axonal tracts during brain development (Berghuis *et al.*, 2007; Mulder *et al.*, 2008; Vitalis *et al.*, 2008; Morozov *et al.*, 2009). During development, the levels of 2-arachidonoylglycerol (2-AG) greatly exceed those of other putative endocannabinoids (e.g. anandamide), suggesting that 2-AG is particularly relevant for developmental processes (Fernandez-Ruiz *et al.*, 2000). 2-AG is mainly synthesized by sn-1 specific diacylglycerol lipases (DGLα and DGLβ) (Bisogno *et al.*, 2003). Monoglyceride lipase (MGL) has been shown to be responsible for ~80% of the catabolism of 2-AG in adult brain (Blankman *et al.*, 2007). These 2-AG synthesizing and degrading enzymes have been found in developing chick (Watson *et al.*, 2008) and mouse (Barabas *et al.*, 2010) brains. To better understand how the ECS affects the development of the reciprocal connections between the cortex and the thalamus, we carefully analyzed the expression patterns of specific ECS components, focusing on regions and developmental stages where the thalamocortical and corticothalamic projections develop and navigate. We generated TCA^{mGFP} mice to visualize, with strong GFP fluorescence, TCAs derived from the three major sensory relay nuclei for the somatosensory, visual, and auditory pathways (see Supplementary Materials for the generation and characterization of TCA^{mGFP} mice). Specifically, immunostaining was conducted to reveal the distributions of CB_1R, DGLβ and MGL in TCA^{mGFP} brains at various embryonic stages to identify the ECS components located in or adjacent to developing TCAs.

At E12.5, CB_1R immunoreactivity was detected in the preplate neurons, in the axonal fibers passing through the intermediate zone of the cortical plate, and in the hippocampal formation (Fig. 5A; n = 1). This staining pattern is similar to the previously reported CB_1R expression profile at this age (Morozov *et al.*, 2009). No CB_1R immunoreactivity was observed in CB_1R KO mice (data not shown). By E14.5, CB_1R positive fibers had reached the PSPB area (Fig. 5B; n = 2). At E16.5, CB_1R positive fibers appeared as fasciculated fiber bundles traversing the striatum and internal capsule (Fig. 5C; n = 2). The developmental pattern of CB_1R positive fibers is similar to the DiI labeled corticothalamic

tracts, which travel through the intermediate zone of the cortical plate, reach and pause at PSPB at E14.5, and arrive at the diencephalon-telencephalon barrier at E16.5 through the internal capsule, suggesting that CB_1 is expressed on elongating axons of the cortical pyramidal neurons.

CB_1R and GFP double-labeling was conducted with E14.5 and E16.5 TCA^{mGFP} brains to reveal the relative relationship between CB_1R-positive fibers and GFP-labeled TCAs (Fig. 5D–I). At E14.5, CB_1R- and GFP-positive fibers from opposite directions meet and intermingle in the PSPB area (Fig. 5D). Close association of GFP and CB_1R immunoreactivity was observed in many individual fascicles (Fig. 5E). At E16.5, both CB_1R- and GFP-positive fibers were found in the striatum (Fig. 5F–H) and fasciculated together as fiber bundles. However, in each bundle, CB_1R- and GFP-positive axons were segregated (Fig. 5H). In the cortical plate, the positive areas for CB_1R and GFP were segregated (Fig. 5F). Previously, it has been reported that thalamocortical fibers are typically well segregated from corticothalamic fibers in the cortical plate: TCAs run through the subplate area and avoid the intermediate or the subventricular zone, while the corticothalamic fibers run through the intermediate zone but not in the subplate (Ohyama *et al.*, 2004). This relationship was reflected by the staining pattern of CB_1R and GFP in TCA^{mGFP} cortical plate at E16.5. CB_1R immunoreactivity was found in the cortical area close to the ventricular wall while GFP was found in an area closer to the marginal zone. By P4, CB_1R was undetectable in the corticothalamic tracts (Fig. 5I), similar to previous report where adult CB1R expression in interneurons is established around postnatal day 5 (Vitalis et al., 2008). In sum, CB_1R is abundantly expressed early in development in corticothalamic axons, but then its levels decline during the early postnatal period.

Next, we examined the expression of DGLβ, a 2-AG synthesizing enzyme, particularly important during development (Bisogno *et al.*, 2003), and MGL, the 2-AG degrading enzyme, in TCA^{mGFP} embryos (Fig. 6). At E14.5, both DGLβ and MGL-positive fibers were observed in the thalamus (Fig. 6B, C; n = 3). They projected ventrally, turned dorsally at the internal capsule, and paused at the PSPB area. MGL positive fibers were also found in the cortical plate, similar to CB_1R immunostaining (Fig. 6C). DGLβ immunoreactivity was mainly co-localized with GFP, and much more rarely with CB_1Rs (Fig. 6D–F), while MGL immunoreactivity co-localized with both GFP and CB_1R (Fig. 6G–I). At E16.5, DGLβ expression remained prominent in the TCAs and was adjacent to CB_1R positive CTAs (Fig6. J–N; n = 3). MGL continued to be expressed in both CB_1R -positive CTAs and GFP-positive TCAs (Fig6. O–Q; n = 3). Thus, the expression pattern of DGLβ during E14–E16.5 is primarily restricted to the TCAs, while MGL is present in both TCAs and CTAs. Taken together, our data suggest that 2-AG is synthesized in the developing TCAs and is degraded in both TCAs and CTAs. This pattern of MGL expression will likely provide fine regulation of 2-AG availability. The close proximity of these two enzymes to CB_1R-positive CTAs suggests that 2-AG could be the endogenous ligand modulating CB_1R-mediated interactions between TCAs and CTAs during axonal fasciculation.

Mice with a cortex-specific deletion of CB_1R also had axon fasciculation and pathfinding deficits

To address if CB_1R expression in corticothalamic tracts is required for TCA patterning, we examined TCA pattern formation in a conditional CB_1R KO mice with ablation of CB_1R in cortical pyramidal neurons driven by NEX-Cre (Monory *et al.*, 2006). L1-NCAM and CTFL double labeling was conducted in E16.5 NEX-driven CB_1R conditional KO (NEX-CB_1R cKO; $CB_1R^{f/f;Nex\text{-}Cre}$; n = 3; were called Glu-CB_1R KO in Monory *et al.*, 2006) and their littermate control mice ($CB_1R^{f/f}$; n = 3) to examine the reciprocal connections between the thalamus and the cortex (Fig. 7. L1) staining revealed fasciculation deficits in the PSPB area and in the deep layer of the cortical plate in NEX-CB_1R cKO (Fig. 7 B1, B2) compared to

their littermate controls (Fig. 7 A1, A2), similar to what we have found in the P0 NEX-CB_1R cKO (see Mulder *et al.*, 2008). Interestingly, CTFL staining revealed a similar degree of TCA fasciculation deficits in NEX-CB_1R cKO (Fig. 7 B3) and total KO mice (Fig. 3). Misrouted TCAs were observed in NEX-CB_1R cKO mice (Fig. 7 B3 and panel 2) but not in their littermate controls (Fig. 7 A3 and panel 1). In sum, fasciculation and pathfinding deficits observed in the NEX-CB_1R cKO mice were reminiscent of those observed in the total CB_1R knockout mice. These data confirm a role for CB_1R in axonal fasciculation, and furthermore suggest that CB_1R signaling in developing CTAs mediates a handshake interaction that instructs the fasciculation process of their complementary connections, the thalamocortical projections.

Discussion

We previously reported that genetic ablation of cannabinoid receptor type 1 (CB_1R) or prenatal CB_1R pharmacological blockade led to abnormal fasciculation in long-range axons, revealed by L1-NCAM and neurofilament M staining (Mulder *et al.*, 2008). In this study we used the developing somatosensory circuit as a model system to examine the role of endocannabinoid signaling in the formation of specific neural circuits. We demonstrated that CB_1R, rather than GPR55 is central to mediating the effects of endocannabinoids on axon fasciculation and pathfinding during development for both corticothalamic axons (CTAs) and thalamocortical axons (TCAs). CTAs harboring CB_1Rs are intimately associated with elongating TCAs, which have very few, if any, CB_1Rs. Immunoreactivity for DGLβ, a 2-AG synthesizing enzyme, is found in the thalamocortical axons while MGL, a 2-AG degrading enzyme, is present in both CTAs and TCAs. Surprisingly, the loss of CB_1Rs in cortical principal neurons leads to aberrant TCA formation. Taken together, we demonstrate for the first time that endocannabinoid signaling is a modulator of the handshake interactions between the TCAs and CTAs, especially for the interactions mediating the fasciculation process. Given the locations of DGLβ and MGL, 2-AG is likely to be the major eCB acting through CB_1Rs in modulating the reciprocal connections between the thalamus and the cortex. Unintentional dysregulation of CB_1R signaling during development is a potential etiology for the mental health disorders linked to prenatal *Cannabis* use.

The role of CB_1R in axonal fasciculation and pathfinding

During nervous system development, axons navigate along stereotyped pathways and fasciculate/defasciculate in distinctive domains along their path (reviewed in Dodd & Jessell, 1988; Van Vactor, 1998). Proper brain wiring requires orchestrated interactions between axon tracts and the environment at distinct domains as well as homo/hetero-philic interactions among axonal fibers. Four major ligand/receptor families involved in axon guidance identified to date include: (1) semaphorins and their plexin and neuropilin receptors, (2) netrins and their DCC and UNC5 receptors, (3) Slits and their roundabout (Robo) receptors, and (4) ephrins and their Eph receptors (reviewed in O'Donnell *et al.*, 2009). Several homo- or hetero-philic cell adhesion molecules (for example, Ig CAMs and cadherins) mediating the fasciculation process have also been identified (Van Vactor, 1998). Mutations of many of these molecules lead to deficits in both axonal pathfinding and fasciculation (for example, see Caras, 1997; Kolk *et al.*, 2009). These observations suggest that axon guidance and axon fasciculation share overlapping sets of signaling pathways. The axonal fasciculation/pathfinding deficits in CB_1R KO mice suggests that CB_1R signaling is likely to modulate one or more of these signaling cascades to properly adjust the coordinated function of cell adhesion molecules during neural circuit formation.

TCA fasciculation deficits have been described in mice heterozygous for the growth-associated protein 43 (GAP43; McIlvain *et al.*, 2003) gene and in mice lacking the gene for the neural cell adhesion molecule L1 (L1-NCAM; Ohyama *et al.*, 2004; Wiencken-Barger *et*

al., 2004). GAP-43 is expressed in neuronal growth cones during brain development and is required for axonal pathfinding (Strittmatter *et al.*, 1995; Maier *et al.*, 1999; Shen *et al.*, 2002; Donovan & McCasland, 2008). Using both DiI tracing and CTFL immunostaining, we found abnormally large thalamocortical fascicles in the striatum and aberrant TCA trajectories in the PSPB area in the developing CB_1R KO brain. This phenotype is highly reminiscent of the axonal deficits found in the GAP43 heterozygous mice (Fig. 4 in McIlvain *et al.*, 2003). We also observed the same phenotype in GAP43 heterozygous mice with CTFL-staining (data not shown). Interestingly, the characteristics of the whisker-related cortical map deficits in CB_1R KO (Deshmukh *et al.*, 2007) and GAP43 heterozygous mutant mice are also similar (McIlvain *et al.*, 2003). The septa area between whisker-related TCA clusters are significantly wider in these two mutant lines compared to their littermate controls. The co-localization of CB_1R with GAP43 and L1 in developing axons suggest that these molecules might act together to regulate axonal fasciculation/pathfinding (Gomez *et al.*, 2008).

ECS signaling modulates the “handshake” between the corticothalamic and thalamocortical axons

Using newly generated TCA reporter mice (TCA^{mGFP}), we were able to demonstrate abundant CB_1R expression in the developing CTAs, while little or no expression was detected in the thalamocortical projections. Surprisingly, TCA development is impaired in both total CB_1R KO mice and in mice with CB_1R specifically deleted from cortical principal neurons. These data indicate that CB_1Rs on the CTAs modulate the fasciculation and axonal pathfinding of the TCAs, their complementary partners.

Most fasciculation aberrancies and pathfinding errors in the TCAs of CB_1R mutant mice occurred as they navigated through the pallial-subpallial boundary (PSPB; also called the striatocortical boundary) area and advanced into the subplate layer of the cortex. The PSPB has been proposed to be a critical region for the development of the reciprocal connections between the thalamus and the cortex, acting as a barrier zone for fibers and a corridor for migrating neurons (Molnar & Butler, 2002). When the rapidly elongating TCAs or CTAs reach the PSPB area, they each pause for a while before exiting this zone. Deleting the transcription factor Pax6 in this area causes many TCAs and CTAs to take aberrant routes (Simpson *et al.*, 2009). In E14.5 TCA^{mGFP} brains, CB_1R-positive fibers were often found closely associated with GFP-positive TCAs (Fig. 6D, G). The presence of DGLβ in this area also indicates the availability of 2-AG to activate CB_1R signaling in CTAs. Complementing the CB_1R expression profile, DGLβ was mainly detected in TCAs with much lower levels in the CTAs. Thus, TCAs may provide 2-AG to activate CB_1Rs on CTAs. In this scheme, 2-AG signaling will be terminated by MGL expressed on both tracts. Recently, 2-AG has been found to be the major eCB modulating synaptic plasticity at mature synapses as well as adult neurogenesis in mice (Tanimura *et al.*, 2010; Gao *et al.*, 2010). We propose that subsequent modulation of cell adhesion molecules triggered by CB_1R then influences the TCA fasciculation process. However, the molecular details of ECS signaling in these “handshake” interactions between TCAs and CTAs remain to be determined.

The “Handshake Hypothesis” has been proposed based on detailed anatomical studies employing carbocyanine dyes demonstrating the close association of the thalamocortical and early corticofugal projections at the PSPB (Molnar & Blakemore, 1995; Molnar *et al.*, 1998a). The observations that thalamic innervations showed an inverted pattern in *reeler* mice, in which the cortical layers were disorganized and developed in an outside-in sequence (Molnar et al., 1998b), and that deleting a particular transcription factor expressed only in the cortex or in the thalamus leads to abnormalities in both CTAs and TCAs (Hevner *et al.*, 2002; Molnar *et al.*, 2003) lend further support to this hypothesis. While the “handshake’ of CTAs and TCAs still occurrs in CB_1R KO and NEX-CB_1R cKO mice, a loss

of CB_1R signaling leads to aberrant axon fasciculation and pathfinding. The TCA fasciculation phenotype observed in the NEX-Cre driven CB_1R conditional KO mice provides strong evidence that the handshake paradigm that governs proper axonal outgrowth and target recognition also governs aspects of the fasciculation process. This is first time that endocannabinoid signaling has been demonstrated to modulate handshake interactions between the TCAs and CTAs.

Implications of ECS signaling in sensory circuit development

In adult brains, CB_1R expression in glutamatergic axonal terminals is relatively low compared to their abundance in GABAergic terminals (for review see Kano *et al.*, 2009). In contrast, CB_1R is highly expressed in developing glutamatergic neurons within the cortical plate and their long-range axonal projections, where they may play a functional role in development (Mulder *et al.*, 2008; Vitalis *et al.*, 2008). Our finding of long-lasting alterations in the development of the glutamatergic connections between the thalamus and the cortex in CB_1R KO mice provides strong evidence to support a role for CB_1Rs in neural circuit formation *in vivo*. It remains to be determined whether these anatomical abnormalities lead to functional deficits in sensory circuits. Recently, Li et al. (2009) found that pharmacological CB_1R blockade in juvenile rats perturbs the functional representations of individual whiskers in the S1 cortex. Thus, it is possible that the abnormally large fascicles and mis-routed TCAs in CB_1R KO mice observed here may affect sensory processing at later ages.

CB_1R expression in human fetal brains (Wang *et al.*, 2003; Mulder *et al.*, 2008) parallels what we and others have seen in rodent brain (Mulder *et al.*, 2008; Vitalis *et al.*, 2008). Δ^9-THC in marijuana smoke readily crosses the placental barrier (Hutchings *et al.*, 1989) and is secreted through breast milk (Perez-Reyes & Wall, 1982). Cannabis is the most widely abused illicit drug worldwide, with greatest abuse occurring between the age of 15–30 years, the peak of reproductive period (Kendler *et al.*, 2008; Tang & Orwin, 2009). Longitudinal human studies have found several behavioral abnormalities in offspring following prenatal marijuana exposure– including exaggerated startle responses and poor habituation to novel stimuli in infants, and hyperactivity, inattention and cognitive deficits in adolescents (Richardson *et al.*, 1995; Fried *et al.*, 2003; Huizink & Mulder, 2006; Galve-Roperh *et al.*, 2009; Jutras-Aswad *et al.*, 2009; Lutz, 2009;; Schneider, 2009). In addition, a number of animal studies have found glutamatergic dysfunction in cannabinoid exposed offspring (Mereu *et al.*, 2003; Antonelli *et al.*, 2004; Antonelli *et al.*, 2005; Campolongo *et al.*, 2007; Castaldo *et al.*, 2007). It is interesting to speculate based on these studies and our current results that Δ^9-THC exposure and engagement of CB_1R leads to alterations in the thalamocortical and corticothalamic projections, and that these might contribute to the behavioral deficits reported in humans.

The present study provides strong evidence that endocannabinoid signaling through CB_1R is an additional mechanism to modulate the development of thalamocortical and corticothalamic circuits. The data reported here have important implications in understanding the long-term consequences of CB_1R disruption in human brain development. Environmental modifications, such as prenatal exposure to exogenous cannabinoids, or compounds that indirectly activate (or desensitize) CB_1Rs, could result in specific developmental alterations of CB_1R signaling that are likely to generate defects in sensory circuits and may have persistent detrimental consequences for sensory or other functions. Unintentional dysregulation of CB_1R signaling during development is a potential neurodevelopmental etiology for the mental health disorders linked to prenatal cannabis exposure.

Supplementary Material

Refer to Web version on PubMed Central for supplementary material.

Acknowledgments

We thank Andrea Conrad for the isolation of CB_1R mutant embryos and Scott Hastings for antibody purifications. GPR55 mice were provided by The Texas Institute for Genomic Medicine. Tau^{mGFP} mice were originally generated by Dr. Silvia Arber and provided to us by Dr. Kaashif A. Ahmad and Dr. Huda Zoghbi. We wish to thank Drs. Shen-Ju Zhou, Cecilia Ljunberg, and Michael Albright for critical reading the manuscript. This work was supported by grants from the National Institutes of Health (NS048884 (HCL), DA021696 (KM) and DA021285 (KM)) and NARSAD (HCL). We also would like to thank Dr. Richard Atkinson for assistance with the confocal microscopy and Baylor IDDRC core facility (NIH HD024064). We would also like to thank Dr. Joanna Jankowsky for providing access to apotome imaging system.

Abbreviations

2-AG	2-arachidonoylglycerol
AA	arachidonic acid
CB_1R	cannabinoid receptor type 1
CB_2R	cannabinoid receptor type 2
cp	cortical plate
CTAs	corticothalamic axons
CTFL	C-erminal full length
cx	cortex
DGL	diacylglycerol lipase
DiI	1,1’-diotadecyl-3,3,3’,3’-etramethylindocarbocyanine
DT	dorsal thalamus
eCBs	endogenous cannabinoids
ECS	endocannabinoid system
ge	ganglionic eminence
hc	hippocampus
HY	hypothalamus
GAP43	growth-associated protein 43
GPCR	G-protein coupled receptor
GPR55	G-protein coupled receptor 55
ic	internal capsule
KO	knockout
L1	L1-NCAM
lv	lateral ventricle
mGFP	membrane-anchored Green Fluorescent Protein
MGL	monoglyceride lipase
PFA	paraformaldehyde

PKC	protein kinase C
PSPB	pallial-subpallial boundary
RT	reticular nucleus
S1	primary somatosensory cortex
st	striatum
TCAs	thalamocortical axons
TE	thalamic eminence
th	thalamus
THC	Δ^9-tetrahydrocannabinol
VT	ventral thalamus

Reference

Agmon A, Connors BW. Thalamocortical responses of mouse somatosensory (barrel) cortex in vitro. Neuroscience. 1991; 41:365–379. [PubMed: 1870696]

Alitto HJ, Usrey WM. Corticothalamic feedback and sensory processing. Curr Opin Neurobiol. 2003; 13:440–445. [PubMed: 12965291]

Antonelli T, Tanganelli S, Tomasini MC, Finetti S, Trabace L, Steardo L, Sabino V, Carratu MR, Cuomo V, Ferraro L. Long-term effects on cortical glutamate release induced by prenatal exposure to the cannabinoid receptor agonist (R)-(+)-[2,3-dihydro-5-methyl-3-(4-morpholinyl-methyl)pyrrolo[1,2,3-de]-1, 4-benzoxazin-6-yl]-1-naphthalenylmethanone: an in vivo microdialysis study in the awake rat. Neuroscience. 2004; 124:367–375. [PubMed: 14980386]

Antonelli T, Tomasini MC, Tattoli M, Cassano T, Tanganelli S, Finetti S, Mazzoni E, Trabace L, Steardo L, Cuomo V, Ferraro L. Prenatal exposure to the CB1 receptor agonist WIN 55,212-2 causes learning disruption associated with impaired cortical NMDA receptor function and emotional reactivity changes in rat offspring. Cereb Cortex. 2005; 15:2013–2020. [PubMed: 15788701]

Barabas K, Keimpema E, Morozov YM, Tortoriello G, Cameron G, Elphick M, Yanagawa Y, Watanabe M, Mackie K, Harkany T. Molecular signature of metabolic networks maintaining protrusive 2-arachidonoyl glycerol signaling during neuronal differentiation. submitted. 2010

Berghuis P, Rajnicek AM, Morozov YM, Ross RA, Mulder J, Urban GM, Monory K, Marsicano G, Matteoli M, Canty A, Irving AJ, Katona I, Yanagawa Y, Rakic P, Lutz B, Mackie K, Harkany T. Hardwiring the brain: endocannabinoids shape neuronal connectivity. Science. 2007; 316:1212–1216. [PubMed: 17525344]

Bisogno T, Howell F, Williams G, Minassi A, Cascio MG, Ligresti A, Matias I, Schiano-Moriello A, Paul P, Williams EJ, Gangadharan U, Hobbs C, Di Marzo V, Doherty P. Cloning of the first sn1-DAG lipases points to the spatial and temporal regulation of endocannabinoid signaling in the brain. J Cell Biol. 2003; 163:463–468. [PubMed: 14610053]

Blankman JL, Simon GM, Cravatt BF. A comprehensive profile of brain enzymes that hydrolyze the endocannabinoid 2-arachidonoylglycerol. Chem Biol. 2007; 14:1347–1356. [PubMed: 18096503]

Campolongo P, Trezza V, Cassano T, Gaetani S, Morgese MG, Ubaldi M, Soverchia L, Antonelli T, Ferraro L, Massi M, Ciccocioppo R, Cuomo V. Perinatal exposure to delta-9-tetrahydrocannabinol causes enduring cognitive deficits associated with alteration of cortical gene expression and neurotransmission in rats. Addict Biol. 2007; 12:485–495. [PubMed: 17578508]

Caras IW. A link between axon guidance and axon fasciculation suggested by studies of the tyrosine kinase receptor EphA5/REK7 and its ligand ephrin-A5/AL-1. Cell Tissue Res. 1997; 290:261–264. [PubMed: 9321687]

Castaldo P, Magi S, Gaetani S, Cassano T, Ferraro L, Antonelli T, Amoroso S, Cuomo V. Prenatal exposure to the cannabinoid receptor agonist WIN 55,212-2 increases glutamate uptake through

overexpression of GLT1 and EAAC1 glutamate transporter subtypes in rat frontal cerebral cortex. Neuropharmacology. 2007; 53:369–378. [PubMed: 17631920]

Chevaleyre V, Takahashi KA, Castillo PE. Endocannabinoid-mediated synaptic plasticity in the CNS. Annu Rev Neurosci. 2006; 29:37–76. [PubMed: 16776579]

Deshmukh S, Onozuka K, Bender KJ, Bender VA, Lutz B, Mackie K, Feldman DE. Postnatal development of cannabinoid receptor type 1 expression in rodent somatosensory cortex. Neuroscience. 2007; 145:279–287. [PubMed: 17210229]

Dinh TP, Carpenter D, Leslie FM, Freund TF, Katona I, Sensi SL, Kathuria S, Piomelli D. Brain monoglyceride lipase participating in endocannabinoid inactivation. Proc Natl Acad Sci U S A. 2002; 99:10819–10824. [PubMed: 12136125]

Dodd J, Jessell TM. Axon guidance and the patterning of neuronal projections in vertebrates. Science. 1988; 242:692–699. [PubMed: 3055291]

Donovan SL, McCasland JS. GAP-43 is critical for normal targeting of thalamocortical and corticothalamic, but not trigeminothalamic axons in the whisker barrel system. Somatosens Mot Res. 2008; 25:33–47. [PubMed: 18344146]

Feldman DE. Synaptic mechanisms for plasticity in neocortex. Annu Rev Neurosci. 2009; 32:33–55. [PubMed: 19400721]

Feldman DE, Brecht M. Map plasticity in somatosensory cortex. Science. 2005; 310:810–815. [PubMed: 16272113]

Fernandez-Ruiz J, Berrendero F, Hernandez ML, Ramos JA. The endogenous cannabinoid system and brain development. Trends Neurosci. 2000; 23:14–20. [PubMed: 10631784]

Freund TF, Katona I, Piomelli D. Role of endogenous cannabinoids in synaptic signaling. Physiol Rev. 2003; 83:1017–1066. [PubMed: 12843414]

Fried PA, Watkinson B, Gray R. Differential effects on cognitive functioning in 13- to 16-year-olds prenatally exposed to cigarettes and marihuana. Neurotoxicol Teratol. 2003; 25:427–436. [PubMed: 12798960]

Fujiyama F, Furuta T, Kaneko T. Immunocytochemical localization of candidates for vesicular glutamate transporters in the rat cerebral cortex. J Comp Neurol. 2001; 435:379–387. [PubMed: 11406819]

Galve-Roperh I, Palazuelos J, Aguado T, Guzman M. The endocannabinoid system and the regulation of neural development: potential implications in psychiatric disorders. Eur Arch Psychiatry Clin Neurosci. 2009; 259:371–382. [PubMed: 19588184]

Gao Y, Vasilyev DV, Goncalves MB, Howell FV, Hobbs C, Reisenberg M, Shen R, Zhang MY, Strassle BW, Lu P, Mark L, Piesla MJ, Deng K, Kouranova EV, Ring RH, Whiteside GT, Bates B, Walsh FS, Williams G, Pangalos MN, Samad TA, Doherty P. Loss of retrograde endocannabinoid signaling and reduced adult neurogenesis in diacylglycerol lipase knock-out mice. J Neurosci. 2010; 30:2017–2024. [PubMed: 20147530]

Garel S, Rubenstein JL. Intermediate targets in formation of topographic projections: inputs from the thalamocortical system. Trends Neurosci. 2004; 27:533–539. [PubMed: 15331235]

Gomez M, Hernandez ML, Pazos MR, Tolon RM, Romero J, Fernandez-Ruiz J. Colocalization of CB1 receptors with L1 and GAP-43 in forebrain white matter regions during fetal rat brain development: evidence for a role of these receptors in axonal growth and guidance. Neuroscience. 2008; 153:687–699. [PubMed: 18400407]

Harkany T, Mackie K, Doherty P. Wiring and firing neuronal networks: endocannabinoids take center stage. Curr Opin Neurobiol. 2008; 18:338–345. [PubMed: 18801434]

Heath CJ, Picciotto MR. Nicotine-induced plasticity during development: modulation of the cholinergic system and long-term consequences for circuits involved in attention and sensory processing. Neuropharmacology. 2009; 56(Suppl 1):254–262. [PubMed: 18692078]

Heintzmann R, Ficz G. Breaking the resolution limit in light microscopy. Brief Funct Genomic Proteomic. 2006; 5:289–301. [PubMed: 17170013]

Hensch TK. Critical period plasticity in local cortical circuits. Nat Rev Neurosci. 2005; 6:877–888. [PubMed: 16261181]

Hevner RF, Miyashita-Lin E, Rubenstein JL. Cortical and thalamic axon pathfinding defects in Tbr1, Gbx2, and Pax6 mutant mice: evidence that cortical and thalamic axons interact and guide each other. J Comp Neurol. 2002; 447:8–17. [PubMed: 11967891]

Hippenmeyer S, Vrieseling E, Sigrist M, Portmann T, Laengle C, Ladle DR, Arber S. A developmental switch in the response of DRG neurons to ETS transcription factor signaling. PLoS Biol. 2005; 3:e159. [PubMed: 15836427]

Huizink AC, Mulder EJ. Maternal smoking, drinking or cannabis use during pregnancy and neurobehavioral and cognitive functioning in human offspring. Neurosci Biobehav Rev. 2006; 30:24–41. [PubMed: 16095697]

Hur EE, Zaborszky L. Vglut2 afferents to the medial prefrontal and primary somatosensory cortices: a combined retrograde tracing in situ hybridization. J Comp Neurol. 2005; 483:351–373. [PubMed: 15682395]

Hutchings DE, Martin BR, Gamagaris Z, Miller N, Fico T. Plasma concentrations of delta-9-tetrahydrocannabinol in dams and fetuses following acute or multiple prenatal dosing in rats. Life Sci. 1989; 44:697–701. [PubMed: 2538691]

Inan M, Crair MC. Development of cortical maps: perspectives from the barrel cortex. Neuroscientist. 2007; 13:49–61. [PubMed: 17229975]

Iversen L. Cannabis and the brain. Brain. 2003; 126:1252–1270. [PubMed: 12764049]

Jacobowitz D, Abbott L. Chemoarchitectonic atlas of the developing mouse brain. CRC Press, Boca Raton. 1998

Jacobs EC, Campagnoni C, Kampf K, Reyes SD, Kalra V, Handley V, Xie YY, Hong-Hu Y, Spreur V, Fisher RS, Campagnoni AT. Visualization of corticofugal projections during early cortical development in a tau-GFP-transgenic mouse. Eur J Neurosci. 2007; 25:17–30. [PubMed: 17241263]

Jones EG. Thalamic circuitry and thalamocortical synchrony. Philos Trans R Soc Lond B Biol Sci. 2002; 357:1659–1673. [PubMed: 12626002]

Jones L, Lopez-Bendito G, Gruss P, Stoykova A, Molnar Z. Pax6 is required for the normal development of the forebrain axonal connections. Development. 2002; 129:5041–5052. [PubMed: 12397112]

Jutras-Aswad D, DiNieri JA, Harkany T, Hurd YL. Neurobiological consequences of maternal cannabis on human fetal development and its neuropsychiatric outcome. Eur Arch Psychiatry Clin Neurosci. 2009; 259:395–412. [PubMed: 19568685]

Kano M, Ohno-Shosaku T, Hashimotodani Y, Uchigashima M, Watanabe M. Endocannabinoid-mediated control of synaptic transmission. Physiol Rev. 2009; 89:309–380. [PubMed: 19126760]

Katz LC, Constantine-Paton M. Relationships between segregated afferents and postsynaptic neurones in the optic tectum of three-eyed frogs. J Neurosci. 1988; 8:3160–3180. [PubMed: 3262721]

Kendler KS, Schmitt E, Aggen SH, Prescott CA. Genetic and environmental influences on alcohol, caffeine, cannabis, and nicotine use from early adolescence to middle adulthood. Arch Gen Psychiatry. 2008; 65:674–682. [PubMed: 18519825]

Kolk SM, Gunput RA, Tran TS, van den Heuvel DM, Prasad AA, Hellemons AJ, Adolfs Y, Ginty DD, Kolodkin AL, Burbach JP, Smidt MP, Pasterkamp RJ. Semaphorin 3F is a bifunctional guidance cue for dopaminergic axons and controls their fasciculation, channeling, rostral growth, and intracortical targeting. J Neurosci. 2009; 29:12542–12557. [PubMed: 19812329]

Lauckner JE, Jensen JB, Chen HY, Lu HC, Hille B, Mackie K. GPR55 is a cannabinoid receptor that increases intracellular calcium and inhibits M current. Proc Natl Acad Sci U S A. 2008; 105:2699–2704. [PubMed: 18263732]

Lauckner JE, Reyes F, Xu C, Hille B, Stella N, Mackie K. Distribution and functional characterization of a novel cannabinoid receptor. Society for Neuroscience Abstract. 2005

Lopez-Bendito G, Chan CH, Mallamaci A, Parnavelas J, Molnar Z. Role of Emx2 in the development of the reciprocal connectivity between cortex and thalamus. J Comp Neurol. 2002; 451:153–169. [PubMed: 12209834]

Lopez-Bendito G, Molnar Z. Thalamocortical development: how are we going to get there? Nat Rev Neurosci. 2003; 4:276–289. [PubMed: 12671644]

Lutz B. Molecular biology of cannabinoid receptors. Prostaglandins Leukot Essent Fatty Acids. 2002; 66:123–142. [PubMed: 12052031]

Lutz B. From molecular neurodevelopment to psychiatry: new insights in mechanisms underlying Cannabis-induced psychosis and schizophrenia. Eur Arch Psychiatry Clin Neurosci. 2009; 259:369–370. [PubMed: 19572159]

Maier DL, Mani S, Donovan SL, Soppet D, Tessarollo L, McCasland JS, Meiri KF. Disrupted cortical map and absence of cortical barrels in growth-associated protein (GAP)-43 knockout mice. Proc Natl Acad Sci U S A. 1999; 96:9397–9402. [PubMed: 10430954]

Marsicano G, Goodenough S, Monory K, Hermann H, Eder M, Cannich A, Azad SC, Cascio MG, Gutierrez SO, van der Stelt M, Lopez-Rodriguez ML, Casanova E, Schutz G, Zieglgansberger W, Di Marzo V, Behl C, Lutz B. CB1 cannabinoid receptors and on-demand defense against excitotoxicity. Science. 2003; 302:84–88. [PubMed: 14526074]

McIlvain VA, Robertson DR, Maimone MM, McCasland JS. Abnormal thalamocortical pathfinding and terminal arbors lead to enlarged barrels in neonatal GAP-43 heterozygous mice. J Comp Neurol. 2003; 462:252–264. [PubMed: 12794747]

Mereu G, Fa M, Ferraro L, Cagiano R, Antonelli T, Tattoli M, Ghiglieri V, Tanganelli S, Gessa GL, Cuomo V. Prenatal exposure to a cannabinoid agonist produces memory deficits linked to dysfunction in hippocampal long-term potentiation and glutamate release. Proc Natl Acad Sci U S A. 2003; 100:4915–4920. [PubMed: 12679519]

Molnar Z, Adams R, Blakemore C. Mechanisms underlying the early establishment of thalamocortical connections in the rat. J Neurosci. 1998a; 18:5723–5745. [PubMed: 9671663]

Molnar Z, Adams R, Goffinet AM, Blakemore C. The role of the first postmitotic cortical cells in the development of thalamocortical innervation in the reeler mouse. J Neurosci. 1998b; 18:5746–5765. [PubMed: 9671664]

Molnar Z, Blakemore C. How do thalamic axons find their way to the cortex? Trends Neurosci. 1995; 18:389–397. [PubMed: 7482804]

Molnar Z, Butler AB. The corticostriatal junction: a crucial region for forebrain development and evolution. Bioessays. 2002; 24:530–541. [PubMed: 12111736]

Molnar Z, Cordery P. Connections between cells of the internal capsule, thalamus, and cerebral cortex in embryonic rat. J Comp Neurol. 1999; 413:1–25. [PubMed: 10464367]

Molnar Z, Higashi S, Lopez-Bendito G. Choreography of early thalamocortical development. Cereb Cortex. 2003; 13:661–669. [PubMed: 12764042]

Monory K, Massa F, Egertova M, Eder M, Blaudzun H, Westenbroek R, Kelsch W, Jacob W, Marsch R, Ekker M, Long J, Rubenstein JL, Goebbels S, Nave KA, During M, Klugmann M, Wolfel B, Dodt HU, Zieglgansberger W, Wotjak CT, Mackie K, Elphick MR, Marsicano G, Lutz B. The endocannabinoid system controls key epileptogenic circuits in the hippocampus. Neuron. 2006; 51:455–466. [PubMed: 16908411]

Morozov YM, Torii M, Rakic P. Origin, early commitment, migratory routes, and destination of cannabinoid type 1 receptor-containing interneurons. Cereb Cortex. 2009; 19(Suppl 1):i78–i89. [PubMed: 19346272]

Mulder J, Aguado T, Keimpema E, Barabas K, Ballester Rosado CJ, Nguyen L, Monory K, Marsicano G, Di Marzo V, Hurd YL, Guillemot F, Mackie K, Lutz B, Guzman M, Lu HC, Galve-Roperh I, Harkany T. Endocannabinoid signaling controls pyramidal cell specification and long-range axon patterning. Proc Natl Acad Sci U S A. 2008; 105:8760–8765. [PubMed: 18562289]

Nahmani M, Erisir A. VGluT2 immunochemistry identifies thalamocortical terminals in layer 4 of adult and developing visual cortex. J Comp Neurol. 2005; 484:458–473. [PubMed: 15770654]

Nakagawa Y, O'Leary DD. Dynamic patterned expression of orphan nuclear receptor genes RORalpha and RORbeta in developing mouse forebrain. Dev Neurosci. 2003; 25:234–244. [PubMed: 12966220]

Navarro M, Rubio P, de Fonseca FR. Behavioural consequences of maternal exposure to natural cannabinoids in rats. Psychopharmacology (Berl). 1995; 122:1–14. [PubMed: 8711059]

Navarro M, Rubio P, Rodriguez de Fonseca F. Sex-dimorphic psychomotor activation after perinatal exposure to (-)-delta 9-tetrahydrocannabinol. An ontogenic study in Wistar rats. Psychopharmacology (Berl). 1994; 116:414–422. [PubMed: 7701042]

O'Donnell M, Chance RK, Bashaw GJ. Axon growth and guidance: receptor regulation and signal transduction. Annu Rev Neurosci. 2009; 32:383–412. [PubMed: 19400716]

Ohyama K, Tan-Takeuchi K, Kutsche M, Schachner M, Uyemura K, Kawamura K. Neural cell adhesion molecule L1 is required for fasciculation and routing of thalamocortical fibres and corticothalamic fibres. Neurosci Res. 2004; 48:471–475. [PubMed: 15041201]

Oka S, Nakajima K, Yamashita A, Kishimoto S, Sugiura T. Identification of GPR55 as a lysophosphatidylinositol receptor. Biochem Biophys Res Commun. 2007; 362:928–934. [PubMed: 17765871]

Perez-Reyes M, Wall ME. Presence of delta9-tetrahydrocannabinol in human milk. N Engl J Med. 1982; 307:819–820. [PubMed: 6287261]

Price DJ, Kennedy H, Dehay C, Zhou L, Mercier M, Jossin Y, Goffinet AM, Tissir F, Blakey D, Molnar Z. The development of cortical connections. Eur J Neurosci. 2006; 23:910–920. [PubMed: 16519656]

Richardson GA, Day NL, Goldschmidt L. Prenatal alcohol, marijuana, and tobacco use: infant mental and motor development. Neurotoxicol Teratol. 1995; 17:479–487. [PubMed: 7565494]

Richardson GA, Ryan C, Willford J, Day NL, Goldschmidt L. Prenatal alcohol and marijuana exposure: effects on neuropsychological outcomes at 10 years. Neurotoxicol Teratol. 2002; 24:309–320. [PubMed: 12009486]

Ryberg E, Larsson N, Sjogren S, Hjorth S, Hermansson N, Leonova J, Elebring T, Nilsson K, Drmota T, Greasley P. The orphan receptor GPR55 is a novel cannabinoid receptor. Br J Pharmacol. 2007 in press.

Schneider M. Cannabis use in pregnancy and early life and its consequences: animal models. Eur Arch Psychiatry Clin Neurosci. 2009; 259:383–393. [PubMed: 19572160]

Shen Y, Mani S, Donovan SL, Schwob JE, Meiri KF. Growth-associated protein-43 is required for commissural axon guidance in the developing vertebrate nervous system. J Neurosci. 2002; 22:239–247. [PubMed: 11756507]

Simpson TI, Pratt T, Mason JO, Price DJ. Normal ventral telencephalic expression of Pax6 is required for normal development of thalamocortical axons in embryonic mice. Neural Dev. 2009; 4:19. [PubMed: 19500363]

Smith AM, Fried PA, Hogan MJ, Cameron I. Effects of prenatal marijuana on response inhibition: an fMRI study of young adults. Neurotoxicol Teratol. 2004; 26:533–542. [PubMed: 15203175]

Smith AM, Fried PA, Hogan MJ, Cameron I. Effects of prenatal marijuana on visuospatial working memory: an fMRI study in young adults. Neurotoxicol Teratol. 2006; 28:286–295. [PubMed: 16473495]

Spano MS, Ellgren M, Wang X, Hurd YL. Prenatal cannabis exposure increases heroin seeking with allostatic changes in limbic enkephalin systems in adulthood. Biol Psychiatry. 2007; 61:554–563. [PubMed: 16876136]

Straiker A, Hu SS, Long JZ, Arnold A, Wager-Miller J, Cravatt BF, Mackie K. Monoacylglycerol lipase limits the duration of endocannabinoid-mediated depolarization-induced suppression of excitation in autaptic hippocampal neurons. Mol Pharmacol. 2009; 76:1220–1227. [PubMed: 19767452]

Strittmatter SM, Fankhauser C, Huang PL, Mashimo H, Fishman MC. Neuronal pathfinding is abnormal in mice lacking the neuronal growth cone protein GAP-43. Cell. 1995; 80:445–452. [PubMed: 7859286]

Sur M, Rubenstein JL. Patterning and plasticity of the cerebral cortex. Science. 2005; 310:805–810. [PubMed: 16272112]

Tang Z, Orwin RG. Marijuana initiation among American youth and its risks as dynamic processes: prospective findings from a national longitudinal study. Subst Use Misuse. 2009; 44:195–211. [PubMed: 19142821]

Tanimura A, Yamazaki M, Hashimotodani Y, Uchigashima M, Kawata S, Abe M, Kita Y, Hashimoto K, Shimizu T, Watanabe M, Sakimura K, Kano M. The endocannabinoid 2-arachidonoylglycerol produced by diacylglycerol lipase alpha mediates retrograde suppression of synaptic transmission. Neuron. 2010; 65:320–327. [PubMed: 20159446]

Temereanca S, Simons DJ. Functional topography of corticothalamic feedback enhances thalamic spatial response tuning in the somatosensory whisker/barrel system. Neuron. 2004; 41:639–651. [PubMed: 14980211]

Theyel BB, Llano DA, Sherman SM. The corticothalamocortical circuit drives higher-order cortex in the mouse. Nat Neurosci. 2010; 13:84–88. [PubMed: 19966840]

Van Vactor D. Adhesion and signaling in axonal fasciculation. Curr Opin Neurobiol. 1998; 8:80–86. [PubMed: 9568395]

Vitalis T, Laine J, Simon A, Roland A, Leterrier C, Lenkei Z. The type 1 cannabinoid receptor is highly expressed in embryonic cortical projection neurons and negatively regulates neurite growth in vitro. Eur J Neurosci. 2008; 28:1705–1718. [PubMed: 18973587]

Waldeck-Weiermair M, Zoratti C, Osibow K, Balenga N, Goessnitzer E, Waldhoer M, Malli R, Graier WF. Integrin clustering enables anandamide-induced Ca2+ signaling in endothelial cells via GPR55 by protection against CB1-receptor-triggered repression. J Cell Sci. 2008; 121:1704–1717. [PubMed: 18445684]

Wang X, Dow-Edwards D, Keller E, Hurd YL. Preferential limbic expression of the cannabinoid receptor mRNA in the human fetal brain. Neuroscience. 2003; 118:681–694. [PubMed: 12710976]

Watson S, Chambers D, Hobbs C, Doherty P, Graham A. The endocannabinoid receptor, CB1, is required for normal axonal growth and fasciculation. Mol Cell Neurosci. 2008; 38:89–97. [PubMed: 18378465]

Welker E, Armstrong-James M, Bronchti G, Qurednik W, Gheorghita-Baechler F, Dubois R, Guernsey DL, Van der Loos H, Neumann PE. Altered sensory processing in the somatosensory cortex of the mouse mutant barrelless. Science. 1996; 271:1864–1867. [PubMed: 8596955]

Wiencken-Barger AE, Mavity-Hudson J, Bartsch U, Schachner M, Casagrande VA. The role of L1 in axon pathfinding and fasciculation. Cereb Cortex. 2004; 14:121–131. [PubMed: 14704209]

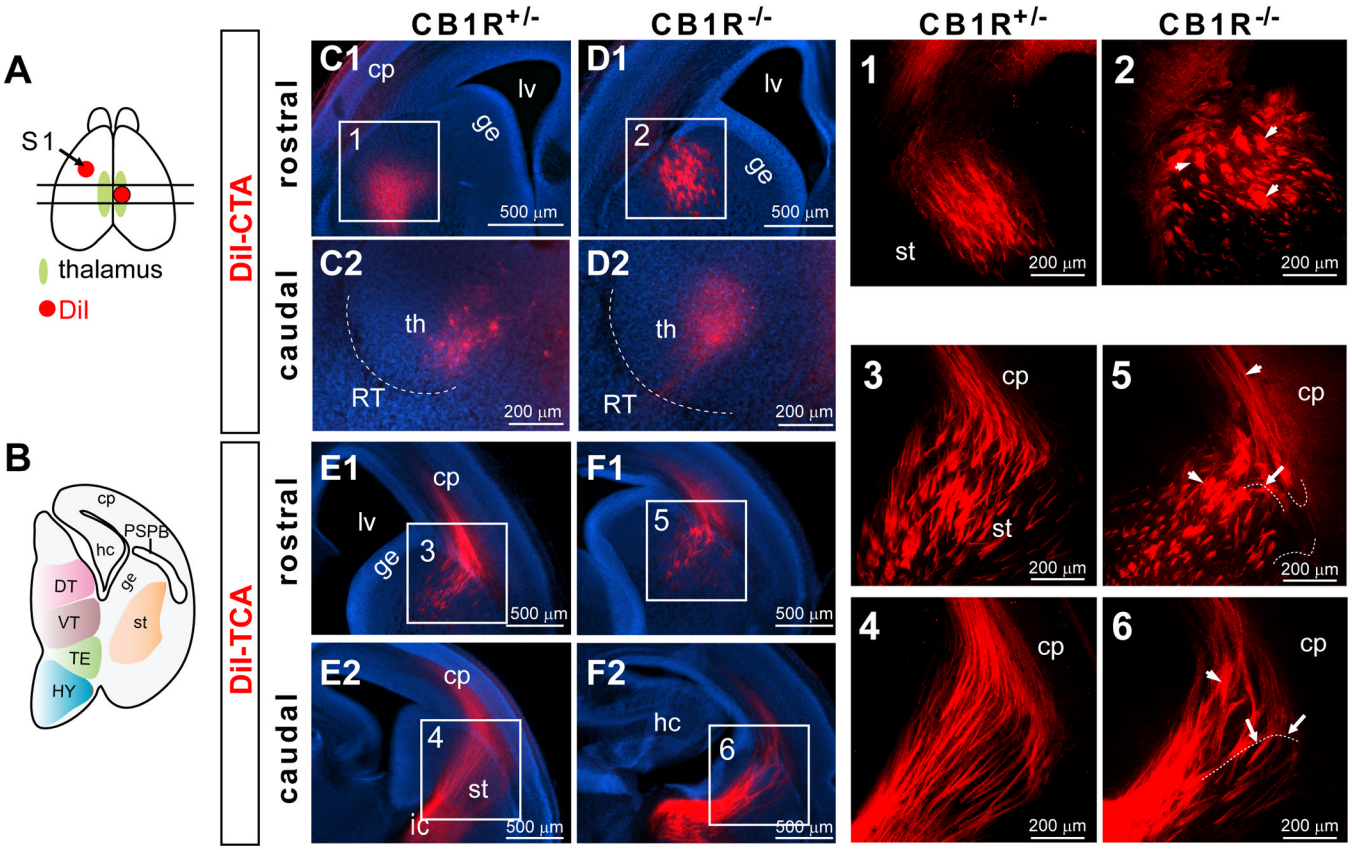

Figure 1. Abnormal fasciculation of corticothalamic and thalamocortical axons in E16.5 CB_1R KO mice

(A) A schematic view illustrates DiI crystal placement in the presumptive S1 area (arrow) of one hemisphere and DiI placement in the dorsal thalamus of the other hemisphere in an E16.5 brain. The two parallel lines indicate the location of two representative planes (rostral and caudal) shown in this figure for each genotype. (**B**) A cartoon illustrates a coronal section taken from the more caudal section indicated in **A**. (**C–D**) The DiI-labeled corticothalamic tracts originating from the S1 cortex cross through the striatum and reach the thalamic nuclei in CB_1R KO (**D**) and littermate control (**C**) mice. Scattered, abnormally large fascicles (arrow heads) were found in CB_1R KO mice (**D1; panel 2**) but not in littermate control mice (**C1; panel 1**). (**E–F**) The DiI-labeled thalamocortical axons pass through internal capsule, the striatum, and target the cortical plate. Several abnormally large fascicles (arrow heads) and misrouted fibers (arrows) were found in CB_1R KO thalamocortical axonal trajectories within the PSPB and cortical plate (**F and panels 5, 6**). (**Panels 1–6**) Projected images of 3-D confocal image stacks for the areas indicated in **C–F**. A few axons have been high-lighted with dashed white lines placed slightly below the fibers as illustrative examples of misrouted axons. Abbreviations: cp, cortical plate; DT, dorsal thalamus; ge, ganglionic eminence; hc, hippocampus; HY, hypothalamus; ic, internal capsule; lv, lateral ventricle; PSPB, the pallial-subpallial boundary; RT, reticular nucleus; S1, primary somatosensory cortex; st, striatum; TE, thalamic eminence; th, thalamus; VT, ventral thalamus.

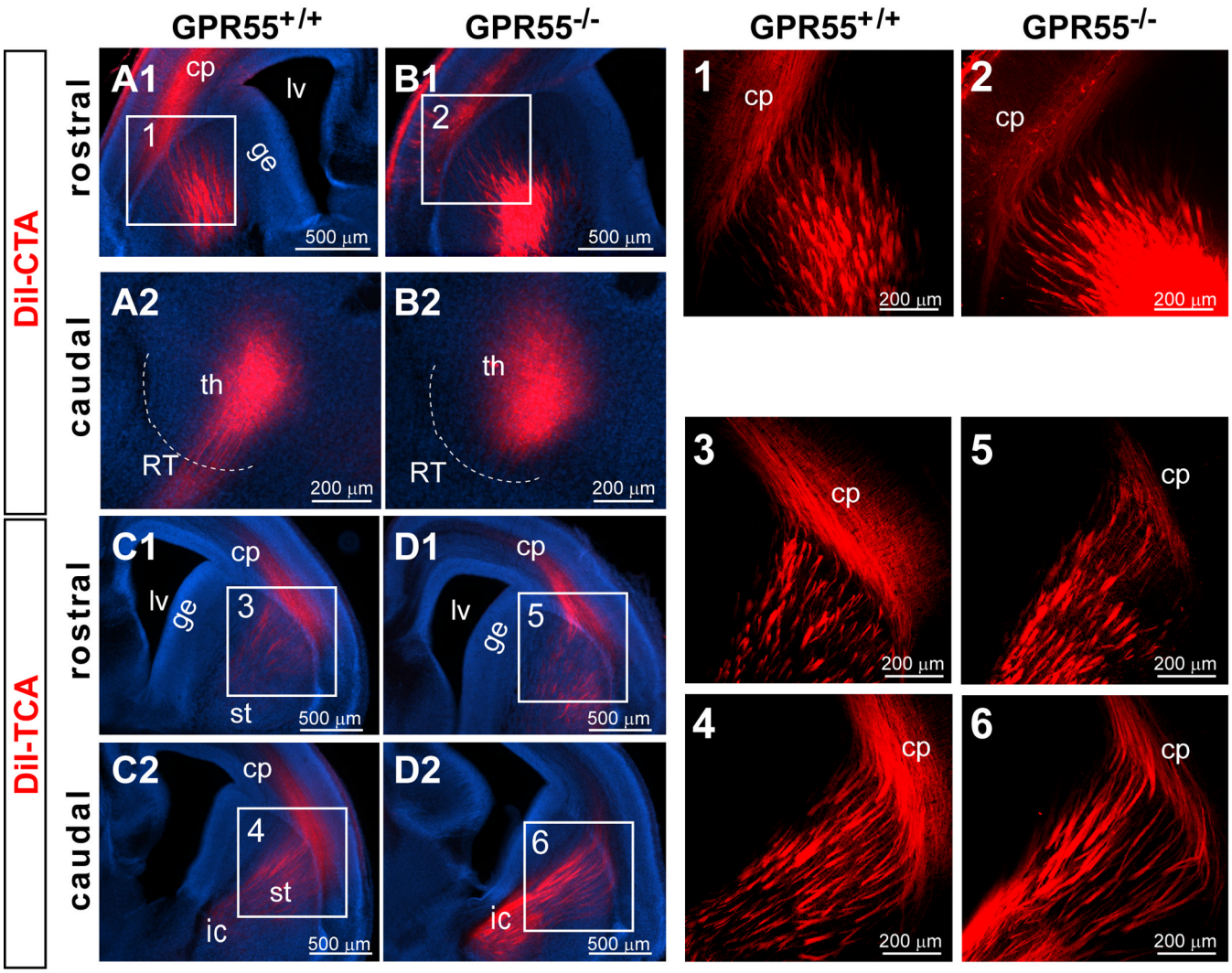

Figure 2. Normal corticothalamic and thalamocortical trajectories in E16.5 GPR55 KO mice

(**A,B**) The DiI-labeled corticothalamic tracts reach the thalamus and the morphology of the axonal tracts appears normal in GPR55 KO mice (**B**) and no different from their wild type littermates (**A**). (**C,D**) DiI-labeled thalamocortical axons target the cortical plate and the axonal fascicles appear normal in the GPR55 KO (**D**), and their littermate control (**C**) mice. (**Panels 1–6)** Projected images of 3-D confocal image stacks for the areas indicated in **A–D**. Abbreviations: cp, cortical plate; ge, ganglionic eminence; ic, internal capsule; lv, lateral ventricle; RT, reticular nucleus; st, striatum.

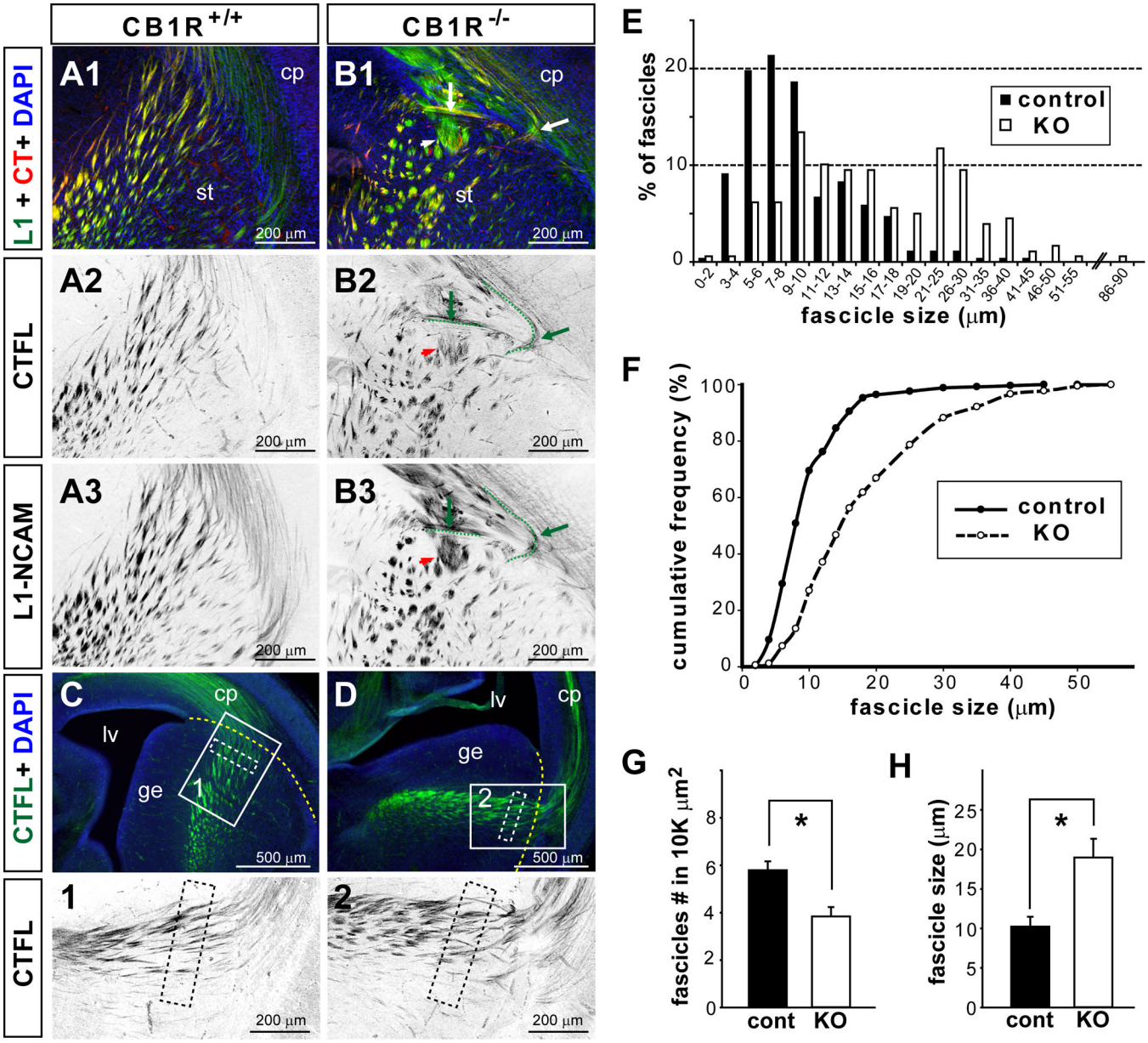

Figure 3. Quantitative difference in fascicle size and number of E16.5 CB_1R KO thalamocortical axons

(A–B) Sample images show L1-NCAM (L1) and CTFL double labeling with coronal brain sections taken from the rostral forebrain areas (as indicated in Figures 1) of control (**A**) and E16.5 CB_1R KO mice (**B**). Aberrant axonal fascicles were detected by both L1 and CTFL immunoreactivity at the PSPB (**B1–B3;** arrows heads indicate large fascicles and arrows indicate misrouted axons; two misrouted axons were high-lighted with dashed green lines placed slightly below the fibers observed). The color of single channel fluorescence images was inverted to provide better illustrations. (**C–H**) The diameter and number of CTFL-positive TCA fascicles were quantified in a 400×100 μm^2 area located in the striatum (white dashed rectangles in **C, D, panels 1–2**) and 100 μm away from the PSPB (yellow dashed lines in **C, D**). These measurements were conducted in 3–5 different PSPB areas per animal and 3 animals per genotype. (**E–H**) Both the diameter and number of TCA fascicles are

significantly different between CB_1R KO and control mice. There was a shift towards larger fascicles in the distribution of thalamocortical axon fascicle size in CB_1R KO mice (**E, F**). The number of fascicles per area measured was significantly reduced (**G**), while the mean fascicle size was significantly increased (**H**) in CB_1R KO mice compared to control. * Student's t-test, $p < 0.05$.

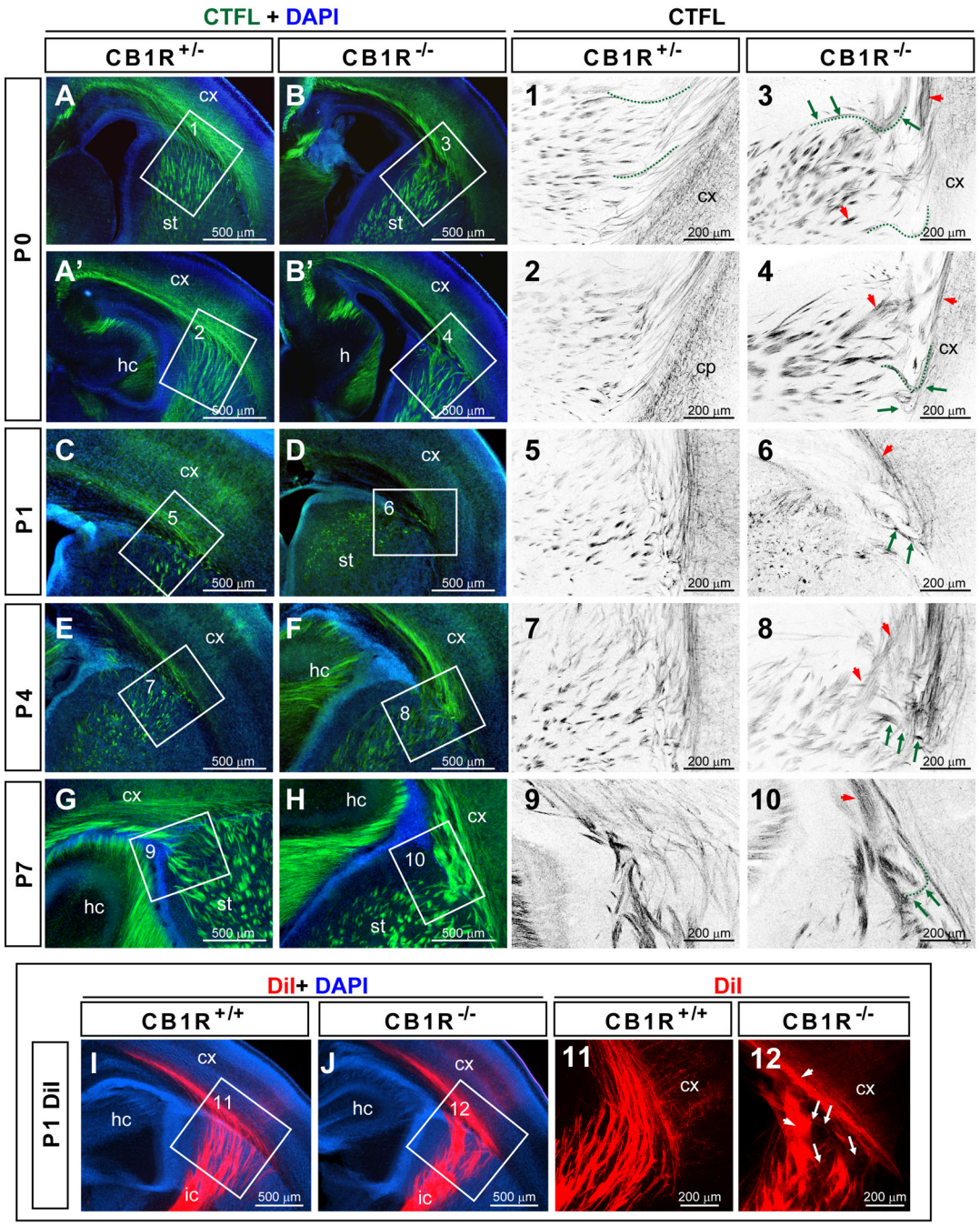

Figure 4. Aberrant thalamocortical axonal fascicles in postnatal CB_1R KO mice

(**A–H**) Representative images of CTFL staining of the TCA distributions in P0, P1, P4 and P7 CB_1R KO and control mice using coronal planes of the rostral forebrain. (**Panels 1–10**) Confocal single plane images indicated in **A–H** by the white rectangles. In these panels, colors have been inverted to better highlight axonal trajectories. Green arrows indicate aberrant axonal trajectories while red arrow heads indicate abnormal fasciculation. A few axons have been high-lighted with dashed green lines placed slightly below the fibers as illustrative examples. Note that the projections of the high-lighted axons from control (panel 1) and CB_1R KO mice were quite different (panel 3). (**I–J**) DiI-labeled TCAs in P1 brains

reveal the aberrant phenotypes in CB_1R KO mice observed with CTFL staining. (**Panels 11–12**) Confocal single plane images indicated in **I–J**. Abbreviations: cx, cortex; hc, hippocampus; ic, internal capsule; st, striatum.

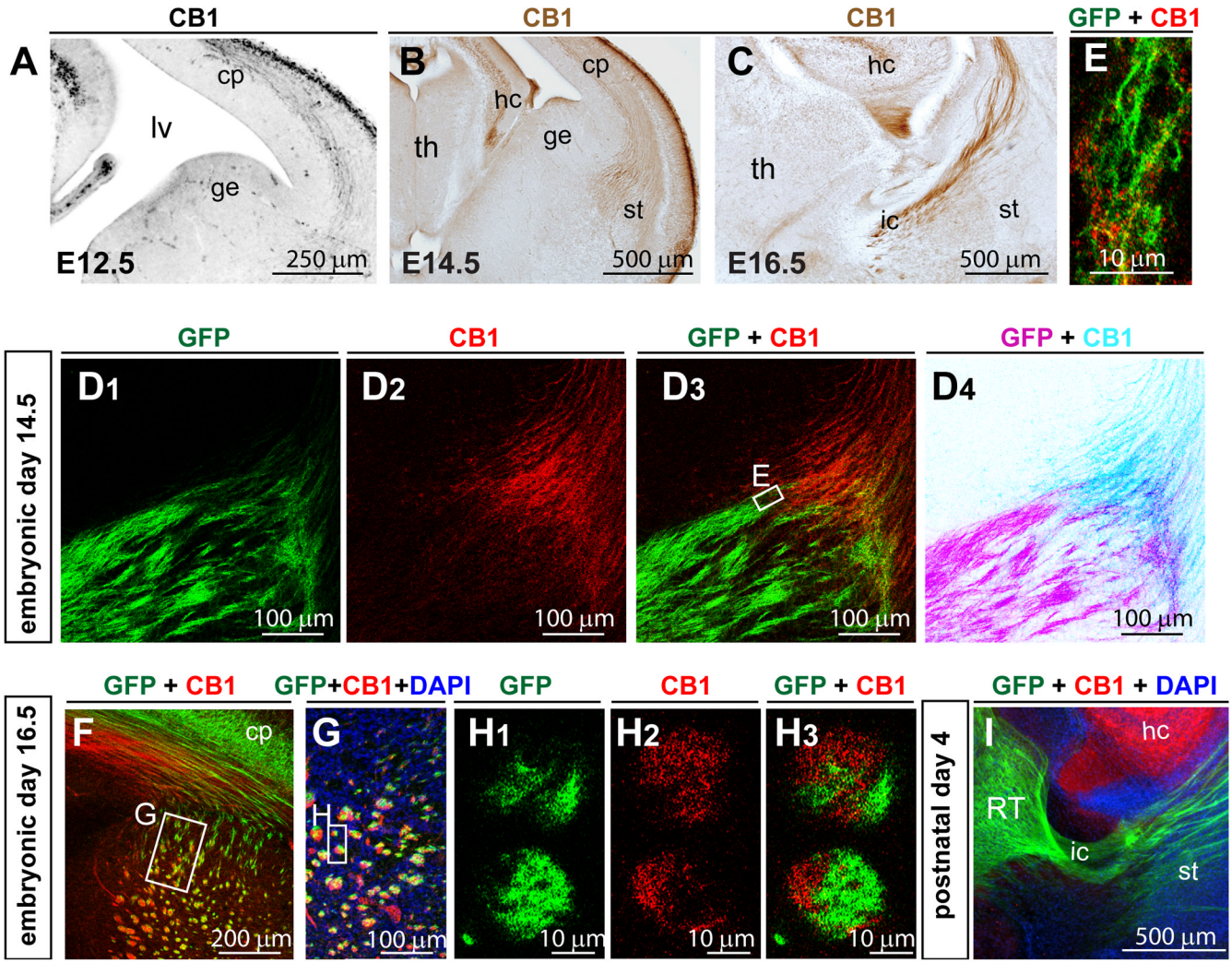

Figure 5. CB_1R is detected in corticothalamic but not in thalamocortical axons during brain development

(**A–C**) CB_1R expression in developing corticothalamic axons at E12.5 (**A**), E14.5 (**B**) and E16.5 (**C**). **A** is the inverted image of fluorescence image. **B, C** are the bright-field images of DAB staining. (**D–I)** Example images of CB_1R and GFP double staining in E14.5 (**D–E**), E16.5 (**F–H**), and P4 (**I**) TCA^{mGFP} mice. In TCA^{mGFP} mice, GFP labels TCAs originating from the primary thalamic relay nuclei. (**D**) At E14.5, CB_1R positive axons and GFP-TCAs meet in the PSPB area and are intermingled in axon bundles (**E**). (**F–H**) By E16.5, CB_1R positive axons have passed through the striatum and internal capsule. (**F–G**) At the striatum and the PSPB in the rostral forebrain region, CB_1R-corticothalamic and GFP-TCA fibers are mingled within the same axon bundles. (**H**) Single confocal plane high magnification images show that CB_1R- and GFP-positive fibers remain segregated within individual axonal bundles. **D4** is the inverted fluorescent images in **D3**. (**I**) By P4, CB_1R expression is down-regulated in axonal tracts, while hippocampal expression remains high. Abbreviations: cp, cortical plate; ge, ganglionic eminence; hc, hippocampus; lv, lateral ventricle; ic, internal capsule; st, striatum; th, thalamus.

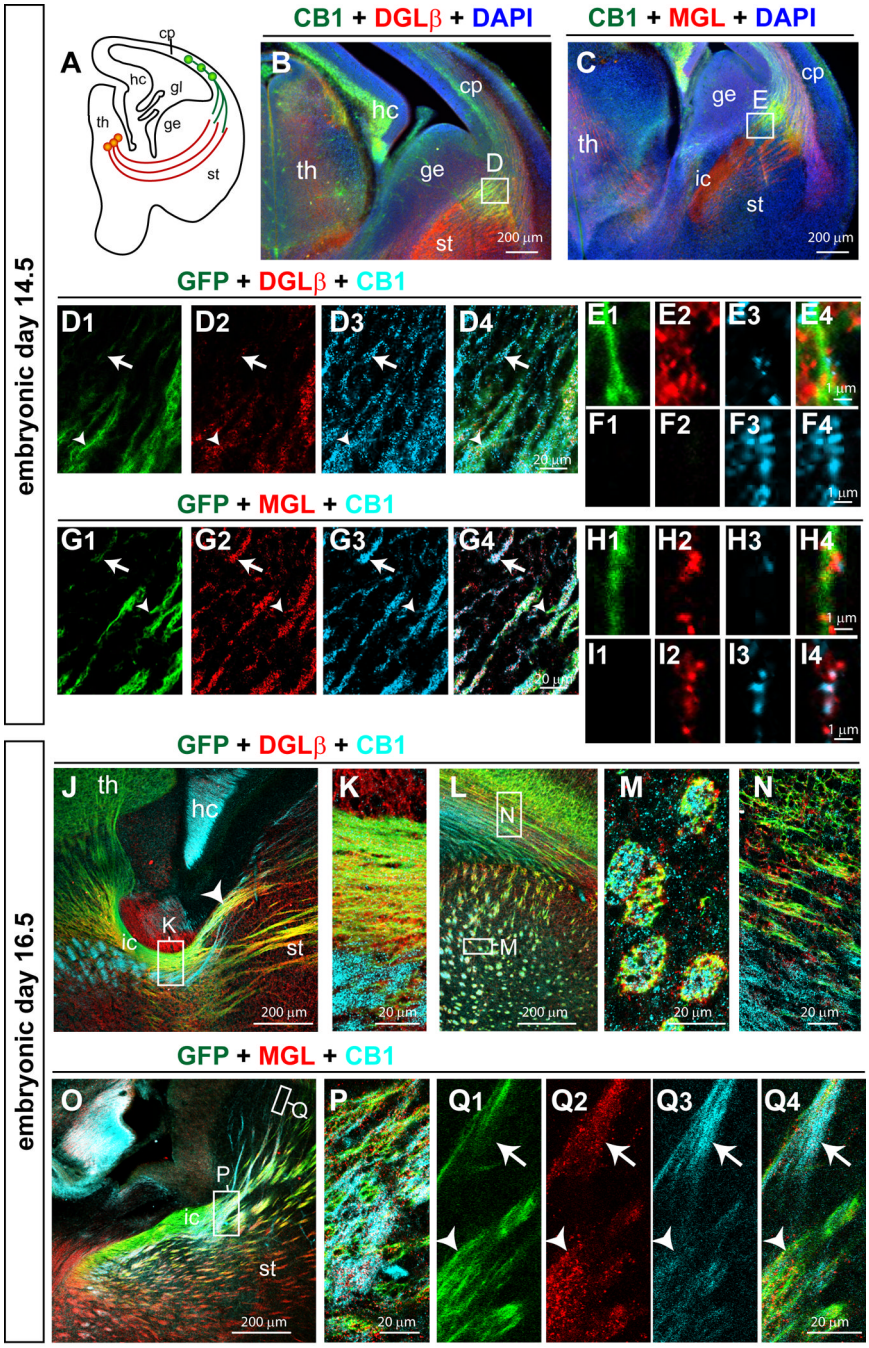

Figure 6. DGLβ and MGL are expressed in developing thalamocortical axonal tracts

(**A**) A schematic diagram shows the distributions of CTAs and TCAs at E14.5. (**B, D**) At E14.5, DGLβ is expressed in GFP-TCAs (arrow heads, **D1, 2, 4, E1–4**), and to a lesser extent in CB_1R-CTAs (arrows, **D2–4, F1–4**). (**C,G**) At E14.5, MGL is located along both GFP-TCAs (arrow heads, **G1, 2, 4, H1–4**) and CB_1R-CTAs (arrows, **G2–4, I1–4**). (**J–N**) At E16.5, DGLβ is located along the GFP-TCAs in the internal capsule (enlarged in **K**) and as the fibers traverse through the striatum (arrow head in **J**). DGLβ is mainly present in GFP-TCAs (yellow in **J–N**) in the striatum, and as the fibers extend within the white matter (**N**). (**O–Q**) At E16.5, a punctate MGL staining pattern was found in both CB_1R-CTAs (arrows)

and GFP-TCAs (arrow heads) as the fibers traversed the striatal region (**Q1–4**) and the internal capsule (**P**). Abbreviations: cp, cortical plate; ge, ganglionic eminence; hc, hippocampus; ic, internal capsule; st, striatum; th, thalamus.

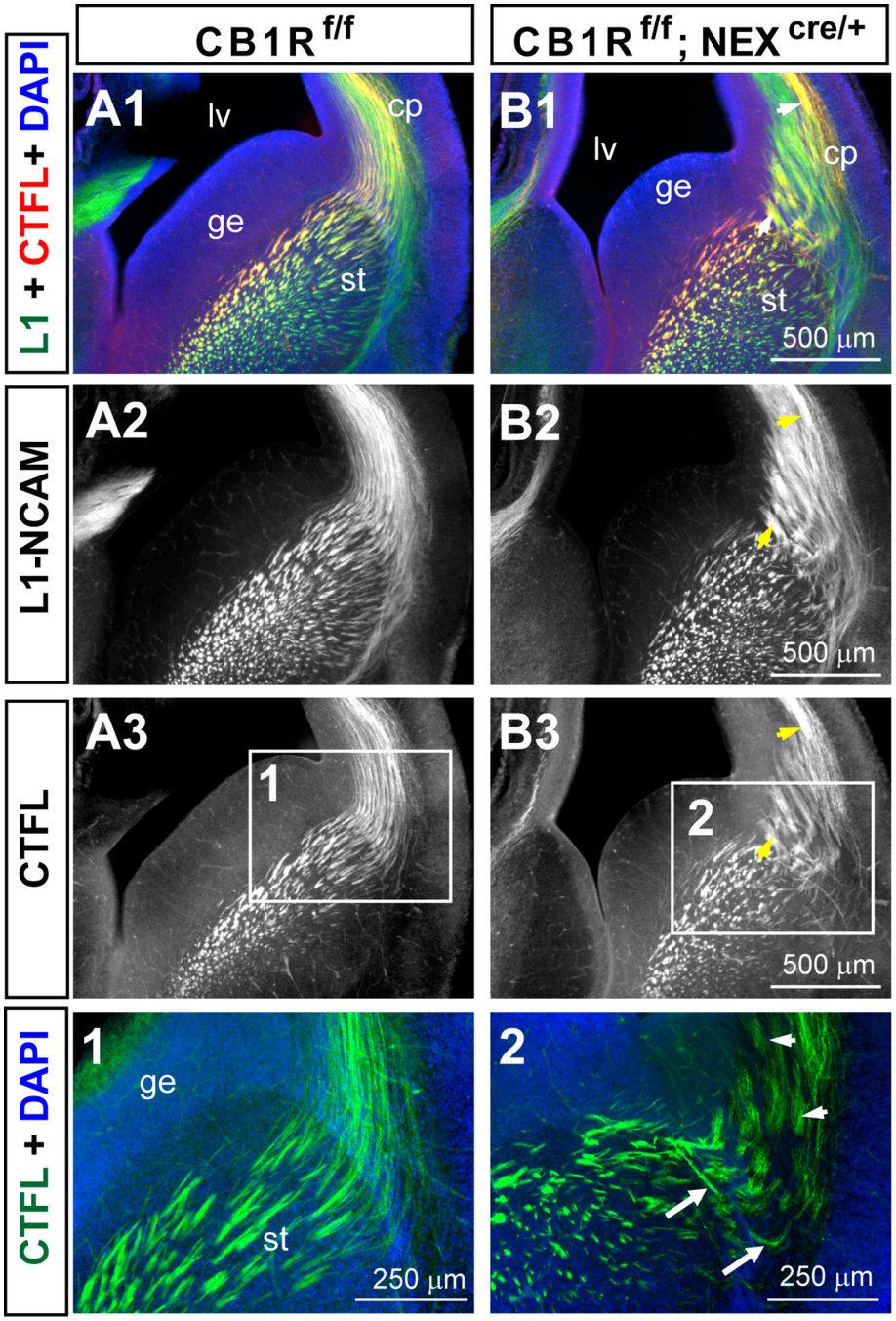

Figure 7. The absence of CB_1R in developing cortical principal neurons leads to abnormal thalamocortical axon tract development

(A–B) Sample images of L1-NCAM and CTFL double staining reveal aberrant fasciculation and axon trajectories in E16.5 NEX-CB_1R cKO (**B**) but not their littermate control mice (**A**). CTFL staining in E16.5 NEX-CB_1R cKO mice (**B3**) revealed abnormal thalamocortical fasciculation and axon trajectories. Arrows point to aberrant axonal trajectories while arrow heads indicate aberrant fasciculation in the mutants. (**Panels 1–2**) Enlarged views of the corresponding areas indicated by the white rectangles in **A3 and B3**. Abbreviations: cp, cortical plate; ge, ganglionic eminence; lv, lateral ventricle; st, striatum.